Functionalized Acenes and Heteroacenes for Organic Electronics

John E. Anthony*

Department of Chemistry, University of Kentucky, Lexington, Kentucky 40506-0055

Received March 30, 2006

Contents

* Phone: 859 257 8844. E-mail: anthony@uky.edu.

1. Introduction

The importance and performance of organic electronic devices have both increased significantly over the last 20 years, evolving from a field with great promise for new materials and applications to a real industry with a few commercial products on the market.[1] Broader acceptance of organic semiconductors will hinge on the development of materials with competitive properties and superior processability, yielding high-performance devices from a significantly less expensive fabrication process.[2] The incorporation of *first-generation* materials into commercial applications has required impressive efforts by physicists and device engineers to yield stable working devices. Efforts by device research groups focused on controlling the morphology of the organic films in these devices and, in many cases, in carefully controlling the degree of crystallinity in the films.[3] The strong correlation between film quality/crystallinity and device performance indicates to the synthetic chemist that the interaction between molecules in the crystalline state is a critical parameter to consider in the development of new materials for electronic applications. Such intermolecular interactions are a particularly important consideration in the design of materials destined to be deposited by solution-based methods, since the typical approach to the solubilization of large aromatic molecules involves the introduction of bulky substituents to at least partially disrupt the strong intermolecular forces that lead to poor solubility.[4] Unfortunately, it is these same intermolecular interactions that also yield desirable electronic properties in many devices.

Efforts to fully understand the relationship between solid-state (or aggregate) order and crystal color/electronic performance intensified with the commercialization of xerography, where differences in charge carrier mobility and efficiency of photogenerated carrier production among similar materials was found to be related to differences in aggregate interactions.[5] One of the earliest theoretical investigations of this issue involved the use of extended Hückel theory in an attempt to relate the precise nature of π-overlap of perylene-based dyes to the color of the crystals.[6] For this class of π-stacked molecules, a strong correlation

10.1021/cr050966z CCC: $59.00
Published on Web 11/23/2006

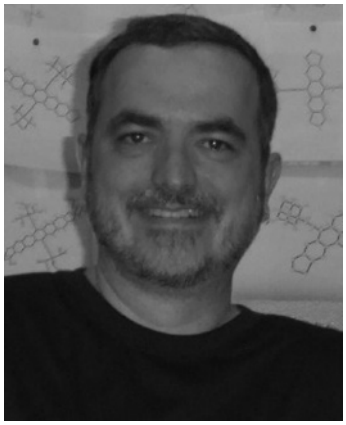

John Anthony was born in Los Angeles' beautiful San Fernando Valley in 1967 and grew up in San Diego. He received his B.A. in Chemistry from Reed College in Portland, Oregon, in 1989 and began his graduate work at UCLA under the direction of Prof. François Diederich in the fall of that year. His research focus was the synthesis of new alkyne-rich compounds for use in the formation of macrocycles and new materials. In 1992, he moved with Prof. Diederich to the Swiss Federal Institute of Technology in Zürich, where he finished his Ph.D. research at the end of 1993. He then moved back to UCLA to perform postdoctoral research with Prof. Yves Rubin, working on rational syntheses of fullerenes. In 1996, he joined the faculty of the University of Kentucky, receiving a Camille and Henry Dreyfus New Faculty Award to begin his career. In 2002, he became the Gill Professor of Chemistry at the University of Kentucky. His research interests include the development of new methods for the synthesis of polycyclic aromatic compounds, their functionalization to improve stability and solubility, and the use of organic semiconductors in electronic devices.

between both longitudinal and transverse intermolecular offset and crystal color was found and was rationalized by considering the overlap of HOMO or LUMO orbitals (and the corresponding nodes) of adjacent molecules. More recently, oligothiophenes,[7] acenes,[8] and heteroacenes[9] have all been subjected to similar studies, at a variety of levels of theory. These studies demonstrated that small changes in intermolecular orientation can lead to significant changes in the electronic properties observed in crystalline solids and emphasized the importance of "molecular engineering" to the development of high-performance electronic materials. This review will highlight the functionalization of linearly fused aromatic systems specifically for their application in electronic devices, with special focus on reports that describe crystal structure/device property relationships in linearly fused acenes and heteroacenes.

1.1. Organic Electronic Devices

Acenes are most commonly exploited in two classes of electronic devices: field-effect transistors (FETs, also known as thin-film transistors, TFTs) and organic light-emitting diodes (OLEDs) (Figure 1). The field-effect transistor device

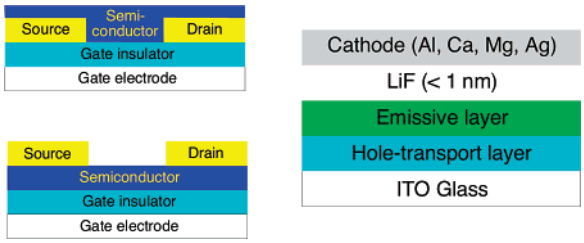

Figure 1. Transistor (left) and light-emitting diode (right) device configurations.

provides detailed information regarding the charge transport properties of the organic material and can be constructed in two common configurations. The bottom-contact device (shown in Figure 1, top left) places the organic semiconductor on top of the source and drain electrodes and is the most convenient platform for the fabrication of solution-processed semiconductor devices. The top-contact device configuration (where the semiconductor lies between the gate dielectric and the source and drain electrodes) typically yields higher performance devices, both because of improved organic film formation on the obstruction-free dielectric surface and due to the superior contact between the source and drain electrodes and the organic semiconductor in a top-contact device. A variety of other factors influence transistor performance, such as the metals used for electrodes, the thickness and nature of the dielectric layer, whether the measurements are carried out in air or under an inert environment, etc.[10] Thus it is important to remember that mobility values for one material can vary by a factor of 2 or more depending on device configuration and measurement conditions.[11] An additional consideration in the fabrication of FETs is the selection of the appropriate electrode material. For p-type semiconductors (where holes, or cations, are the dominant carrier), the work function of the metal must match the energy of the HOMO for the organic semiconductor. Likewise, for n-type semiconductors the work function of the electrode must match the LUMO energy of the organic molecule. Because there are relatively few metals used in transistors (with gold being the most common), it is common for the synthetic chemist to try to improve the interaction between the organic compound and the gold electrode by tuning the oxidation potential (and thus, the HOMO energy level) of the organic species.

The key parameters extracted from organic FET devices are the carrier mobility (μ), the on/off current ratio ($I_{on/off}$), and the threshold voltage (V_{th}). Mobility is one of the most commonly reported benchmarks and is essentially the drift velocity of the charge carrier (cm/s) per unit applied field (V/cm), leading to the units for mobility of $cm^2/(V\ s)$. The on/off current ratio (the difference in source/drain current in the "on" and "off" states) is often related to the purity of the semiconductor, with only highly pure materials yielding low ($<10^{-11}$ A) off currents. Threshold voltage is the voltage at which the transistor turns from the "off" to the "on" state, and is a strong indicator of the quality of the interface between the organic semiconductor and the gate insulator. To be competitive with amorphous silicon in electronic devices, mobility needs to be on the order of 0.5 $cm^2/(V\ s)$ or greater, the on/off current ratio should be at least 10^5, and V_{th} should be as close to 0 as possible. In general, aromatic compounds (and particularly acenes) exhibit almost exclusively hole transport. In cases where electron mobility can be measured, it is typically significantly smaller than the hole mobility measured in similar compounds.

Organic light-emitting diodes (OLEDs, Figure 1, right) serve as the emissive component in organic-based displays. These devices are typically fabricated on substrates of glass coated with a transparent conductor (indium-doped tin oxide, ITO). The bottom layer of most OLEDs is a hole transport layer, to facilitate the oxidation of the emissive layer by the ITO anode. The emissive layer is comprised of an electroluminescent molecule, typically an organic system with high fluorescence quantum yield. Often this layer is capped with an electron-transport layer; alternatively, a thin lithium fluoride layer can be added to improve the interface with

the cathode material. The cathode is typically a low work function metal (aluminum, magnesium, even calcium), to facilitate injection of electrons into the device. Modern OLEDs have good brightness at low power consumption levels: the most significant issue still to be overcome for commercialization is device lifetime and durability.

1.2. Common Acene Packing Motifs

A key to electronic performance in all organic electronic devices is the intermolecular order adopted by the individual molecules in the solid state. In general, good electronic performance requires strong electronic coupling between adjacent molecules in the solid. As will be seen in the body of this review, there are two common packing motifs adopted by acenes and heteroacenes in the solid state that yield strong intermolecular overlap. In the classic "herringbone" arrangement, the aromatic edge-to-face interaction dominates, yielding two-dimensional electronic interactions in the solid (Figure 2, top). Alternatively, the molecules can adopt a

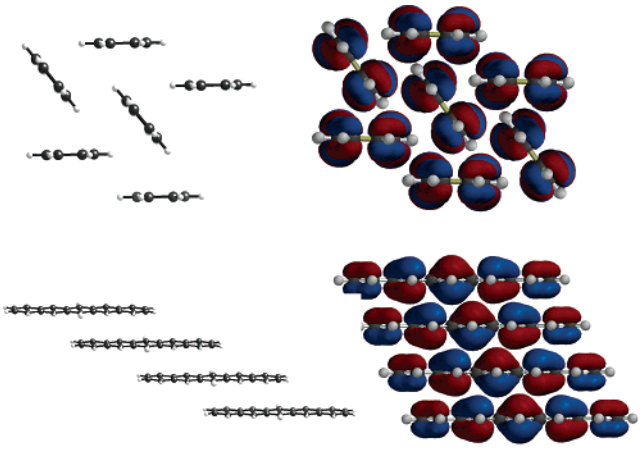

Figure 2. Herringbone (top) and π-stacking (bottom) arrangements of acenes, showing HOMO orbital interactions (Spartan '04, Wavefunction, Inc.).

coplanar arrangement and stack, typically with some degree of displacement along the long and short axes of the molecules (Figure 2, bottom).[12] The strong interaction between the π-electron-rich faces (π-faces) of the molecules in these π-stacked arrays yields strong electronic coupling, and further interactions with adjacent stacks can yield two-dimensional electronic coupling in the solid.

2. Functionalized Anthracenes

2.1. Anthracene Derivatives in Field-Effect Transistors

Anthracene's high oxidation potential, small π-surface, and high fluorescence quantum yield usually relegate materials based on this aromatic core to applications in light-emitting systems. However, recent reports of functionalized anthracenes have placed derivatives of this compound within the realm of materials used for organic field-effect transistors. One of the simplest examples was reported in 2003, consisting of a series of anthracene dimers and trimers that were then subjected to detailed device and morphological studies (Chart 1).[13] The covalent linking of anthracene units

Chart 1

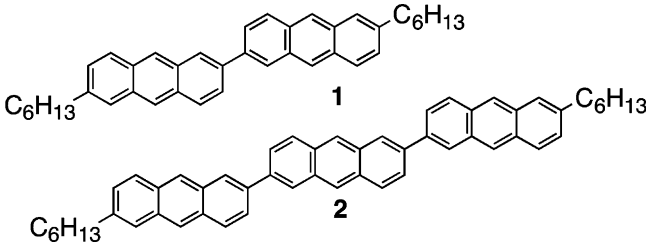

decreases the oxidation potential of the molecule (thus aiding charge injection from the device electrode), while simultaneously increasing potential area of intermolecular overlap. While the X-ray crystal structure for these compounds was not reported, X-ray diffraction (XRD) analysis of thin films shows similarity to other extended aromatic systems that adopt a herringbone arrangement in the solid state. The hole mobility of **2** was measured as 0.18 $cm^2/(V\ s)$, with an on/off current ratio of 10^4. Unfortunately, these values could only be attained when the material was deposited on a substrate held at 175 °C, a temperature that precludes the use of many flexible substrates.

Yamashita and co-workers more recently reported the synthesis and characterization of a simpler series of 2,6-diarylanthracenes (Figure 3).[14] X-ray crystallographic analysis of **3** showed that these molecules favor edge-to-face interactions in the solid, adopting the typical acene herringbone arrangement, with mobility for **4a** measured at 0.004 $cm^2/(V\ s)$ for a vapor-deposited film of this material.[15] Although the substituents do not radically alter the solid-state order of these materials compared with unsubstituted anthracene, they do have a profound effect on the electronic properties of the material. For example, anthracene functionalized with electron-withdrawing 4-trifluoromethylphenyl groups (**3**) behaves as an n-type semiconductor, with FET devices fabricated from vacuum-deposited films showing *electron* mobility as high as 0.003 $cm^2/(V\ s)$. While this mobility value is not high, the use of anthracene as the core of the semiconductor imparts significant stability advantages over larger acenes such as tetracene and pentacene, and this

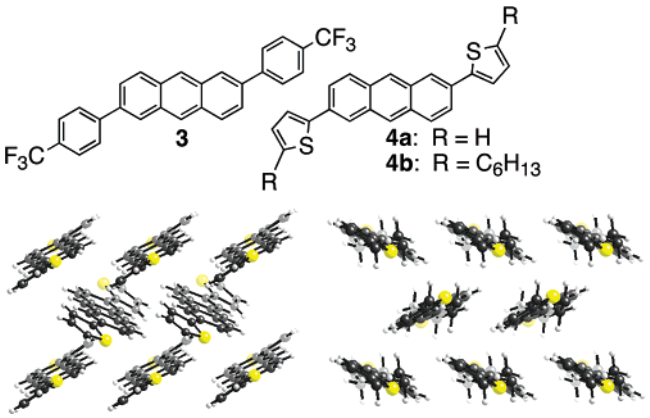

Figure 3. Aryl-substituted anthracenes **3**, **4a**, and **4b**. Views of the crystal packing of **4a** and **4b** show closer face-to-face contacts for **4b**, although the packing is still dominated by edge-to-face interactions (Graphics produced from data stored at the Cambridge Structural Database (CSD) RefCode FINZAE (**4a**) and FINZET (**4b**)).

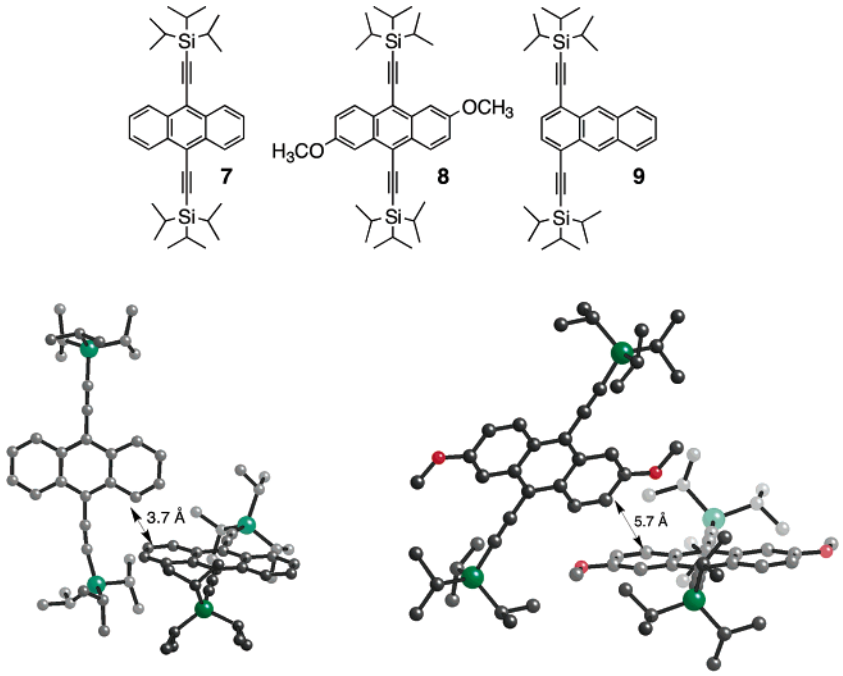

Figure 4. Silylethyne-functionalized anthracene derivatives for OLED applications (top) and the crystal packing of **7** and **8** (bottom).

approach may prove useful in applications where durability, rather than performance, is the deciding factor.

Another report of the synthesis and characterization of **4a** (along with alkyl-substituted **4b)** showed that significantly improved device performance could be achieved by optimizing the deposition conditions.[16] For the simple dithienylanthracene **4a**, FET devices showed a hole mobility of 0.06 $cm^2/(V\ s)$ and on/off current ratios of 10^5. The addition of alkyl groups led to material with significantly improved performance, both due to the improved morphology of the films and due to the subtle change in packing of the molecules, leading to both edge-to-face and face-to-face (closest face-to-face contact = 3.54 Å) interactions. Evaporated thin films of **4b** showed hole mobility as high as 0.5 $cm^2/(V\ s)$, with excellent device stability.

2.2. Anthracene Derivatives in Light-Emitting Diodes

More often, the anthracene chromophore is used for its fluorescence characteristics, where any significant electronic interaction in the solid leads to an undesired broadening of the emission spectrum and a decrease in fluorescence yield. In this case, bulky substituents at the 9,10-positions are typically employed to break up aggregation in the solid state, and a myriad of such compounds have been reported in the literature.[17] One benchmark material among these compounds is the 1-naphthyl-substituted derivative **5** (Chart 2), where

Chart 2

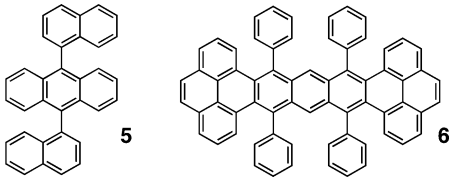

the rigid substituents effectively isolate the chromophore in the solid, yielding an amorphous compound with efficient blue electroluminescence.[18] Because all of these materials are designed to be amorphous (in order to minimize issues with crystal grain boundaries leading to irregular illumination across the device), significant crystallographic studies of solid-state interactions are typically not performed.

One recent example of a unique acene derivative for use in electroluminescent applications is compound **6**.[19] This material, consisting of seven linearly fused aromatic rings, is essentially an anthracene core sandwiched between two pyrene units. The aryl substituents on the central anthracene portion of the molecule cause the aromatic backbone to twist significantly out of planarity, giving this class of materials the common name "twistacenes", while the pyrene units improve the fluorescence quantum yield of the material. The twist of the aromatic backbone, along with the steric bulk of the phenyl substituents, eliminate significant aryl−aryl close contacts in the crystal, making them excellent candidates for use in OLEDs. Indeed, single-layer devices fabricated from **6** (as a dopant in a polyfluorene polymer) yielded high-luminance *white-light*-emitting OLEDs, constituting a key technological breakthrough for the development of organic systems for ambient room lighting or display back-lighting.[20]

An alternative to creating amorphous materials to minimize aromatic interactions in the solid state is to design molecules that crystallize with their chromophores completely isolated by electronically insulating functional groups. One such compound is triisopropylsilylethynyl derivative **7**, for which X-ray crystallographic analysis showed the closest $C_{Ar}-C_{Ar}$ contact is 3.7 Å (Figure 4).

Crystalline films of this material incorporated into a simple OLED structure (Figure 1) yield devices with bright blue emission.[21] The devices reach a maximum emission of 1000 Cd/m^2 and, at a common display intensity of 100 Cd/m^2 (requiring a bias of 7.8 V), produce 1.7 Cd/A. Substitution of **7** with two methoxy groups increases the $C_{Ar}-C_{Ar}$ close-contact to 5.7 Å, and while the light yield at 100 Cd/m^2 for compound **8** is roughly the same as that for **7** (1.4 Cd/A), the voltage, and thus power, required to attain this brightness level is significantly lower (7.0 V). Offsetting the functional

group of **7** to the 1,4-positions (**9**) exposes significantly more π-surface. The resulting material is an amorphous glass, which formed working (but inefficient, 0.4 Cd/A at a brightness of 100 Cd/m^2) devices that showed weak green emission. Examination of the electroluminence spectra of **7** and **9** (Figure 5) demonstrates the detrimental effect of solid-state aromatic interactions on OLED devices, leading to broadened emission and significantly reduced device efficiency.

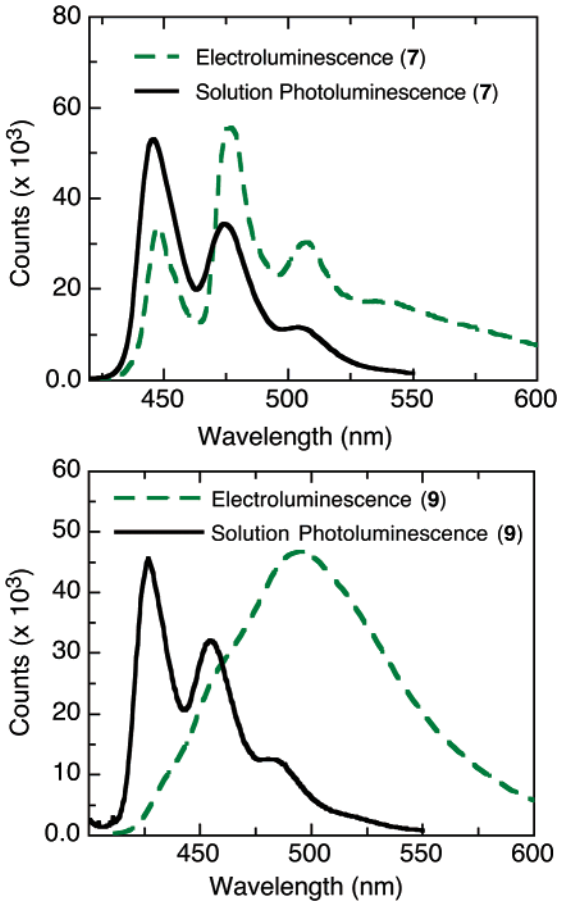

Figure 5. Solution photoluminescence and thin-film electroluminescence spectra of anthracene derivatives **7** and **9**.

2.3. Heteroanthracenes for Organic Transistors

In marked contrast to the relatively few examples of transistor applications of anthracene derivatives, heteroanthracenes (throughout this review, the term "heteroacene" will refer to acene derivatives where a carbocyclic ring or rings have been replaced by a heteroaromatic ring) constitute one of the most common classes of small-molecule semiconducting materials. Just as with anthracene, two different approaches to the functionalization of these compounds have been explored, the formation of dimeric (or trimeric) heteroanthracene derivatives and the functionalization of heteroanthracenes with aryl substituents.

2.3.1. Benzodithiophenes

One of the earliest reports of a high-mobility organic semiconductor described the synthesis and characterization of benzodithiophene dimer **10** (Chart 3).[22] This material exhibited high air stability and reasonable thin-film device properties (μ = 0.04 cm^2/(V s) from a vacuum-deposited film of **10**). To further probe substituent effects in this class of materials, alkyl-substituted derivatives **11** and **12** were prepared, although the alkyl groups used were not sufficient to provide good solubility in any solvent.[23] These derivatives arrange in the crystalline state with significant face-to-face interactions, and compound **11** forms vacuum-deposited films with mobility of 0.016 cm^2/(V s). Extending the conjugation of **10** by functionalization with alkylthienyl groups (**12**) significantly decreased the solubility of the molecule without improving device performance (μ = 0.001 cm^2/(V s) for a vacuum-deposited film).

Chart 3

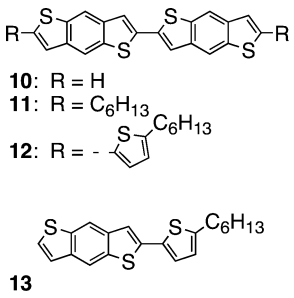

As with anthracene derivatives **3** and **4**, heteroanthracenes functionalized with simple aryl substituents have also proved successful in forming functioning thin-film transistors. One of the earliest reports involved benzodithiophene functionalized with a single alkylthienyl group (**13**, Chart 3).[23] This highly soluble compound yielded uniform films from solution, and chlorobenzene-cast films of **13** showed hole mobility as high as 1.2 $\times$ 10^{-3} cm^2/(V s).

Further developing the class of functionalized benzodi(chalcogenophene)s, Takimiya and co-workers synthesized, characterized, and fabricated transistor devices from the series of diphenyl derivatives shown in Figure 6.[24] The best performing of these compounds, the diphenyl benzodiselenophene **15**, yields FET hole mobility as high as 0.17 cm^2/(V s) from a vacuum deposited film. Crystallographic analysis of this compound revealed that the phenyl substituents are coplanar with the heteroacene and that the material packs with extensive edge-to-face interactions similar to unsubstituted pentacene, with a herringbone angle of 64° (compared with pentacene's herringbone angle of 53°). The high polarizability of the selenium atoms likely contributes strongly to this molecule's ability to undergo electric-field doping, leading to the relatively high observed mobility.

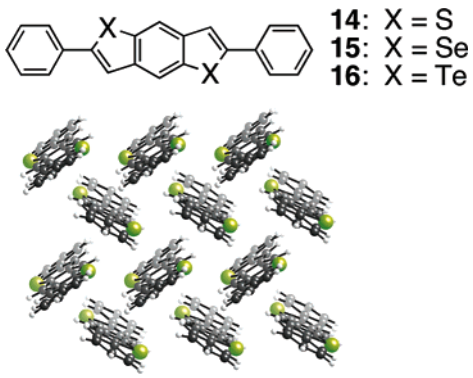

Figure 6. Diphenyldi(chalgogenophene)s **14**−**16** and the crystal packing of compound **15** (CSD RefCode AXICUF), showing herringbone arrangement of the molecules in the crystal.

2.3.2. Dithienothiophene

Further increasing the heteroatom content of benzodithiophenes yields the fully heterocyclic dithienothiophene unit. Bis(dithienothiophene) **17**, a dimerized version of dithienothiophene, is an excellent early example of heteroacene-based organic semiconductors.[25] Crystallographic analysis of this compound showed that the molecules possess strong face-to-face and edge-to-face interactions in the solid state, with interplanar contacts as short as 3.5 Å, and sulfur−sulfur contacts as close as 3.4 Å (Figure 7).[26] Hole mobility

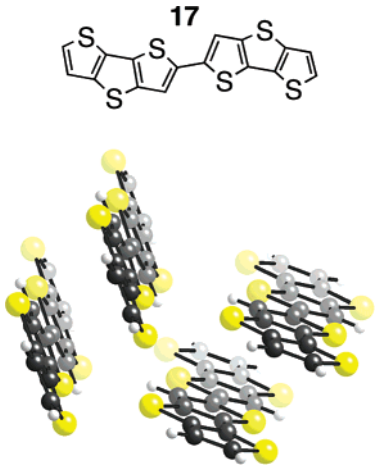

Figure 7. Dimeric dithienothiophene **17** and its crystal packing (CSD RefCode NOBJET), showing significant face-to-face and edge-to-face interactions.

as high as 0.05 $cm^2/(V\ s)$ was measured in top-contact transistors fabricated from evaporated films of **17**, and these devices also exhibited impressive on/off current ratios (10^8), attributed to the large HOMO−LUMO gap of the material (which renders the compound less susceptible to oxidative degradation, yielding fewer impurities). These results were an important demonstration of the utility of heteroacenes, and over the past few years the dithienothiophene core has become a common building block in organic electronics. This system is at the heart of a variety of soluble organic semiconductors, including derivatives exhibiting high field-effect mobility[27] and derivatives that yield light-emitting transistors.[28]

3. Tetracene

Tetracene, like all unfunctionalized acenes, adopts an edge-to-face herringbone arrangement in the solid state (Figure 8).[29] Tetracene provides an interesting illustration of the

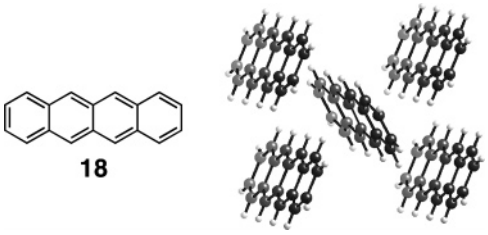

Figure 8. Tetracene structure and packing (RefCode TETCEN01 from CSD), showing predominant edge-to-face orientation.

tradeoff between stability and device performance; it is less stable than anthracene but decomposes in air or light at a significantly slower rate than pentacene (due to tetracene's higher oxidation potential and slower rate of photodimerization). Recent studies on solubilized tetracene derivatives have confirmed that a major photodecomposition pathway is photodimerization, forming the so-called "butterfly" dimer.[30] However, unlike similar dimers of pentacene, the tetracene dimers will convert slowly back to the tetracene monomers in solution.

Tetracene has been used in the construction of FETs with hole mobility as high as 0.1 $cm^2/(V\ s)$[31] and has recently been paired with C_{60} to yield a solar cell with power conversion efficiency of 2.3%.[32] Due to the ability of this molecule to form large, high-quality crystals by vapor growth methods,[33] tetracene has been much more thoroughly studied in single-crystal devices, where hole mobilities as high as 1.3 $cm^2/(V\ s)$ have been reported from devices fabricated directly on the tetracene crystal surface.[34] Studying devices formed on the surface of high-quality crystals allows the determination of properties on material that is as defect-free as possible and is crucial to understanding the intrinsic charge-transport and electronic properties of organic solids.[35]

3.1. Tetracene Derivatives in Organic Transistors

3.1.1. Halogenated Tetracene

The halogenation of tetracene disrupts edge-to-face interactions and induces a shift from the traditional herringbone motif to arrangements with significant face-to-face interactions.[36] Bao and co-workers performed an elegant study showing that mono-halo tetracene derivatives **19** and **20** adopted an approximate sandwich-herringbone arrangement in the crystal (where a pair of molecules adopt face-to-face interactions, then interact in an edge-to-face fashion with other molecule pairs), while the dihalo derivative 5,11-dichlorotetracene **21** packed with extensive long-range π-overlap (Figure 9).[37] The molecules' crystalline order had

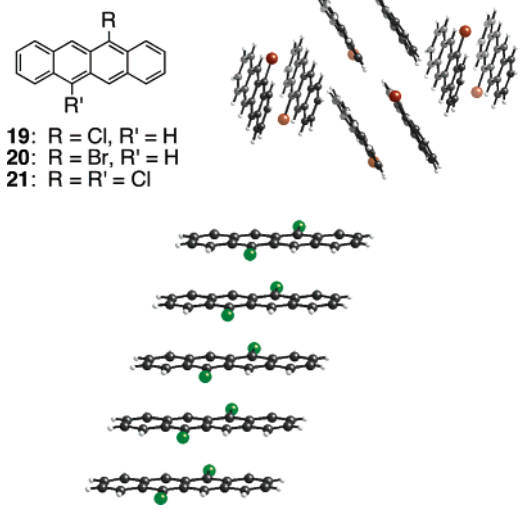

Figure 9. Halogenated tetracenes **19**−**21** and representative crystalline order of compounds **20** (approximate sandwich herringbone) and **21** (columnar π-stacked) (RefCodes FAHTIS and FAHTOY from the CSD).

significant impact on device performance, with devices fabricated on single crystals of the π-stacking **21** yielding hole mobility (1.6 $cm^2/(V\ s)$) as much as 3 orders of magnitude higher than that found in sandwich-herringbone **19** and even slightly higher than mobility typically found in

similar devices made on crystals of unsubstituted tetracene. In stark contrast, devices fabricated from evaporated thin films of **21** had field-effect mobilities less than 0.001 $cm^2/(V\ s)$ due to the poor morphology of the evaporated films. These results underscore both the importance of face-to-face interactions for high intrinsic carrier mobility and the importance of higher-dimensional interactions for the formation to technologically important thin-film devices. This work also demonstrates the ease with which face-to-face interactions can be introduced by appropriate functionalization.

3.1.2. Tetracenes with Polar Substituents

An alternative approach to inducing π-stacking in tetracene derivatives was reported by Nuckolls and co-workers, who prepared a series of 1,4-acenequinones—essentially, acenes with strongly electron-withdrawing groups at only one end.[38] These molecules naturally possess a significant dipole, and crystallographic analysis of the 1,4-pentacenequinone **22** revealed an extended π-stacked array with alternating dipoles in the solid state (Figure 10). The separation between π-faces

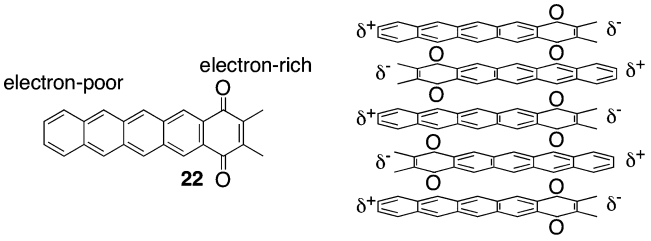

Figure 10. Exploitation of dipolar interactions to induce π-stacking in acenequinones.

within the stack was a remarkably small 3.25 Å, well within the van der Waals radius of the carbon atoms (3.4 Å). FET devices fabricated from the corresponding hexacenequinone had a measured hole mobility of 0.05 $cm^2/(V\ s)$ and excellent device stability. This series of molecules constitutes a unique approach to inducing face-to-face interaction in acenes by exploiting electronic, rather than steric, interactions.

The Nuckolls group has also reported the synthesis and device study of 2,3-dihydroxytetracene **23**, which was found to bind with oxide surfaces such as HfO_2, ZrO_2, and Al_2O_3 (presumably by ester formation).[39] For monolayer surfaces of **23** formed on alumina, X-ray reflectivity measurements demonstrated that the molecules were oriented vertically and were tightly packed on the surface (Figure 11). Because

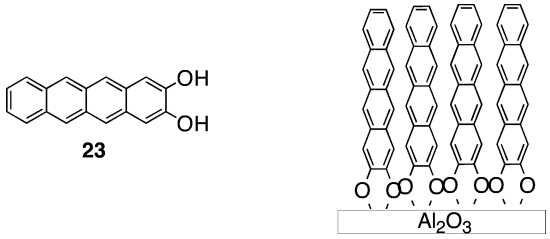

Figure 11. 2,3-Dihydroxytetracene **23** and its close-packed self-assembly on an alumina surface.

alumina is a common gate dielectric used in FETs, a device was constructed using a *single monolayer* of **23** as the semiconducting layer. While these nanoscale monolayer devices were not ideal transistors, they did show gate-voltage-dependent conductivity and demonstrated a promising technique for the fabrication of self-assembled transistors or sensors.

3.1.3. Tetracene–Thiophene Hybrid Materials

Furthering the strategy used for functionalized anthracenes (the addition of aryl substituents to decrease oxidation potential and increase total area of π-overlap), an innovative series of acene−thiophene hybrid semiconductors was recently prepared (Chart 4).[40] Detailed analysis of vapor-

Chart 4

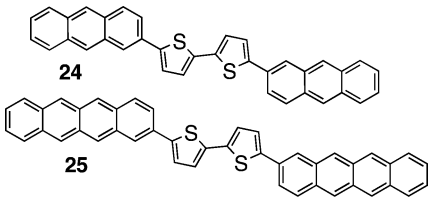

deposited thin films of these materials yielded the unit cell parameters and showed that the molecules stand with their long axes almost perfectly perpendicular to the substrate surface. The tetracene derivative **25** in particular showed high transistor mobility (0.5 $cm^2/(V\ s)$), along with high thermal and oxidative stability.

3.1.4. Rubrene

One of the most intensively studied tetracene derivatives is undoubtedly rubrene (5,6,11,12-tetraphenyl tetracene **26**, Figure 12). This material forms very high quality crystals

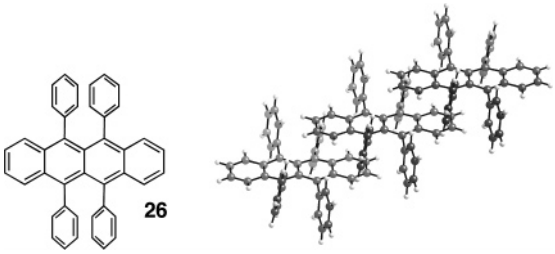

Figure 12. Rubrene **26** and its crystalline order (RefCode QQQCIG from the CSD).

by vapor transport growth methods, and is the current "gold standard" for the study of intrinsic transport properties in organic crystals.[41] Phenyl substitution of tetracene in this case leads to a strongly π-stacked arrangement in the solid state, and computational studies have shown that the particular intermolecular arrangement adopted by rubrene happens to be optimal for charge transport.[42] The highest room-temperature mobility measured for rubrene crystals to-date is 20 $cm^2/(V\ s)$,[43] and rubrene is the first organic material in which accurate Hall measurements have been made, showing directly the density of mobile carriers in the transistor channel, as well as their intrinsic mobility.[44] Ambipolar transport (measurable mobility for both holes and electrons) has also been reported recently in devices fabricated on rubrene single crystals.[45]

Interestingly, thermally evaporated rubrene films do not yield high-performance transistors, typically due to the difficulty in growing high-quality crystalline films of rubrene in the proper polymorphic form.[46] A recent detailed study of this issue showed that, in general, functionalized aromatic compounds that have significantly different vapor phase and solid-state conformations will not easily form highly crystalline films.[47] An interesting and potentially groundbreaking approach to the formation of rubrene-based thin-film transistors utilizes rubrene-doped polymers.[48] A mixture of 9,10-

Scheme 1. Synthesis of Gel-Forming 2,3-Dialkoxytetracene 27

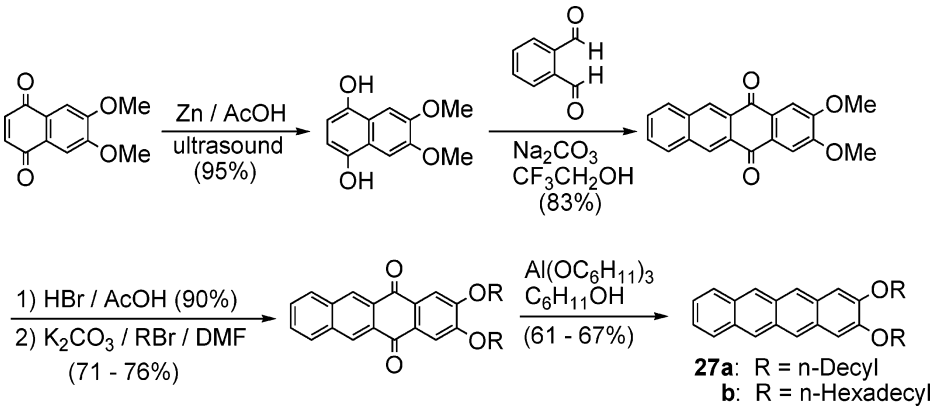

diphenylanthracene, rubrene, and polystyrene, when deposited on a bottom-contact FET substrate and thermally annealed, yielded devices with hole mobility as high as 0.7 $cm^2/(V\ s)$. The ability to combine the high intrinsic mobility of small-molecule aromatic semiconductors with the film-forming ability of high molecular weight polymers is one potential approach to the long-anticipated capability of forming high performance devices by simple solution-processing methods.

3.1.5. Alkyl- and Alkoxy-Functionalized Tetracene

A recent report of the synthesis and study of 2,3-dialkoxy tetracenes (Scheme 1) showed that such molecules form surprisingly robust gels.[49] A strong red shift of the absorption edge for the tetracene chromophore, coupled with significant hypochromism of the ^1L_b band, indicate that the tetracene units in the gel are in close contact and that there is some alignment of the long axes of these molecules. The use of long alkyl chains to align the chromophores may allow the use of such materials in solution-cast semiconducting devices. A similar approach has been used to prepare analogous derivatives of pentacene,[50] leading to self-assembled fibers with unusual optical properties.[51]

A recent report from Swager and co-workers detailed the synthesis and crystallographic analysis of a series of tetracene derivatives, each possessing one aromatic ring substituted with four fluorine atoms and one ring with a long-chain alkyl or alkoxy group (Chart 5).[52] All of these derivatives showed

Chart 5

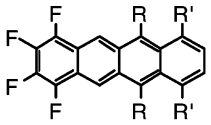

28a: R = H, R' = OC_6H_{13}
28b: R = OC_6H_{13}, R' = H
28c: R = H, R' = C_8H_{17}
28d: R = C_8H_{17}, R' = H

strong π-stacking interactions in the solid state, with face-to-face distances as short as 3.18 Å. Derivative **28c** was unique in this series as the only compound showing strong 2-D π-stacking interactions, a common feature among materials exhibiting high mobility in thin-film devices. The authors report that electronic characterization of these materials is underway.

3.2. Heterotetracenes for Organic Transistors

Extending their work with benzodiselenophenes, Takimiya and co-workers reported the synthesis of two derivatives of benzoselenopheno benzoselenophenes **29** and **30** (Chart 6).[53]

Chart 6

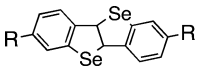

29: R = H
30: R = Phenyl

Both of these compounds packed in a herringbone arrangement similar to pentacene, with herringbone angles of 63° and 58° for **29** and **30**, respectively. Importantly, compound **30** also exhibits some close face-to-face interactions (3.39 Å) between the aromatic carbons in adjacent molecules (notably, there are no Se−Se close contacts between molecules in the crystal). Mobility measured from vacuum-evaporated films of **30** was as high as 0.31 $cm^2/(V\ s)$, and the devices showed very high operational stability.

3.3. Tetracene Derivatives in Organic Light-Emitting Diodes (OLEDs)

While tetracene itself has not found widespread use in OLEDs (since its emission wavelength is blue-shifted from that necessary for saturated green emission),[54] the high hole mobility of tetracene films, coupled with reasonably high fluorescence quantum yield, makes tetracene an ideal semiconductor of light-emitting field-effect transistors.[55] Light emission from these devices is low, making them unsuitable for display applications, but data gleaned from electroluminescence in these devices can provide many details about electronic processes taking place in the semiconductor channel.[56] For display applications, however, tetracene must be functionalized to emit light at a useful wavelength, typically by adding substituents to lower the energy of the fluorescence and yield red emission. Because the highly conjugated substituents required to induce such a significant bathochromic shift provide significant π-surface for strong solid-state interactions, the materials must be further substituted with bulky insulating groups to prevent such electronic communication in the solid. Only a few functionalized tetracenes for red OLEDs have been presented, and the only derivative to yield reasonable red emission was compound **31** (Figure 13).[57]

4. Pentacene

While rubrene sets the performance standard for single-crystal devices, pentacene is the benchmark for thin-film devices. Like its lower homologues, pentacene crystallizes

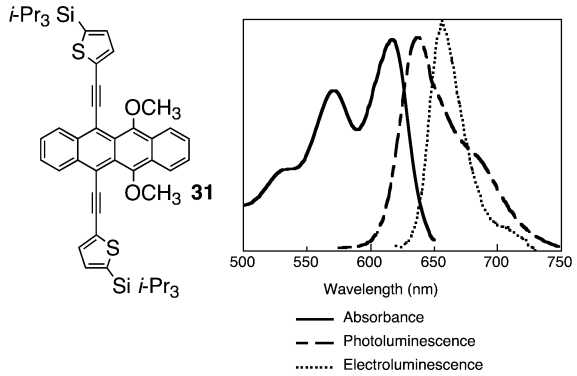

Figure 13. Red-emitting tetracene derivative **31** and its absorption, emission, and electroluminescence spectra.

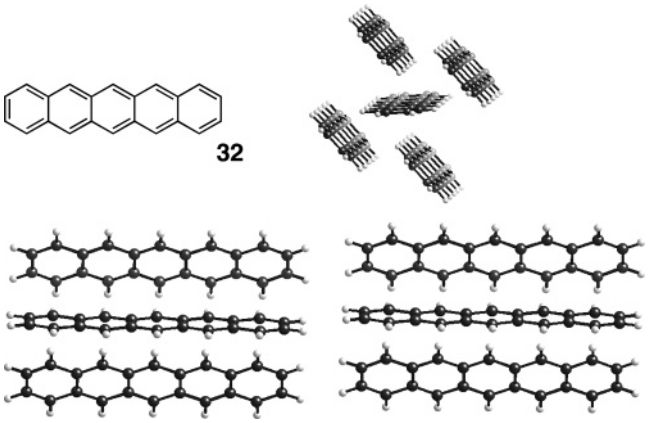

Figure 14. Pentacene and its crystal packing (RefCode PENCEN01 from the CSD), showing predominant 2-D edge-to-face interactions and weak interactions between the ends of the acenes.

in the classic acene herringbone motif (Figure 14),[58] although it can potentially adopt any of a number of polymorphs.[59] This polymorphic nature further complicates device studies, since band structure calculations have shown significant electronic differences between polymorphic forms.[60] These issues have instigated numerous studies of nucleation and film formation during vapor deposition of pentacene,[61] as well as intensive studies of surface treatments to improve the quality of vapor-deposited films.[62] High-quality FET devices made from thin films of pentacene typically show mobilities greater than 1.5 $cm^2/(V\ s)$,[63] values as high as 5 $cm^2/(V\ s)$ have been reported,[64] and ambipolar charge transport has been observed in pentacene thin films (although electron mobilities were very low and n-type behavior was only observed under vacuum).[65] Pentacene has also been used as the p-type material in organic solar cells (with C_{60} as the n-type material), yielding power conversion efficiencies as high as 2.7%.[66]

4.1. Pentacene Derivatives for Transistors

4.1.1. Alkyl- and Halogen-Functionalized Pentacene

The first functionalized pentacene studied for transistor applications was 2,3,9,10-tetramethyl pentacene **33** (Figure 15).[67] This material crystallizes in a herringbone arrangement almost identical to that adopted by unsubstituted pentacene, the only substantial difference being an increase in separation of the pentacene units along the crystallographic *c* axis due to the interposing methyl groups. While the crystal packing changed little, methyl substitution led to significant decrease in oxidation potential versus unsubstituted pentacene, which

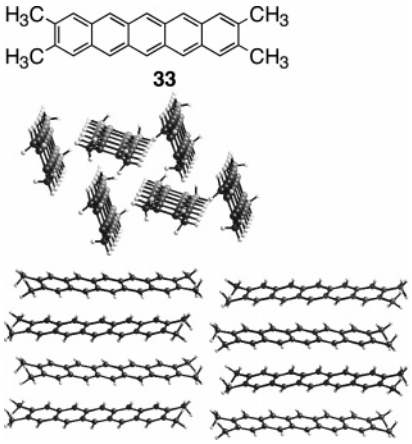

Figure 15. 2,3,9,10-Tetramethyl pentacene **33** and its crystalline order (CSD RefCode ASEPUJ), showing 2-D edge-to-face interactions (center) and increased spacing between pentacene ends (bottom) caused by the methyl functional groups.

should lead to improved charge injection into the organic material from gold electrodes. Devices made from thermally evaporated films of **33** show hole mobilities as high as 0.3 $cm^2/(V\ s)$, with on−off current ratios of 6×10^3.

Another functionalization strategy that strongly influences both the electronic and intermolecular ordering properties of pentacene is perfluorination. Suzuki and co-workers reported an impressive synthesis of perfluoropentacene **34** (prepared in five steps from tetrafluorophthalic anhydride and hydroquinone) and performed detailed characterization of its device performance.[68] Compound **34** crystallized in a herringbone motif similar to that adopted by pentacene but with a nearly 90° edge-to-face angle (compared with 52° for pentacene) and closer contact between the pentacene rings (as close as 3.25 Å, Figure 16). Transistor devices fabricated

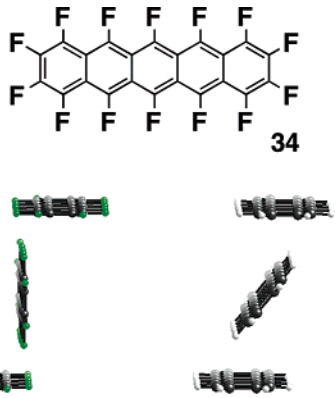

Figure 16. Perfluoro pentacene **34** and its edge-to-face interactions (bottom left, CSD RefCode BEZLUO) compared with those of pentacene **32** (bottom right, RefCode PENCEN01).

from this compound exhibited electron mobilities as high as 0.22 $cm^2/(V\ s)$, demonstrating that perfluorination is a viable route to prepare n-type semiconductors from acenes. This same research group has also reported the synthesis and characterization of perfluorotetracene, although carrier mobility in this compound was not as impressive as that seen in **34**.[69]

4.1.2. Aryl-Functionalized Pentacenes for Organic Transistors

The addition of simple phenyl substituents to the *peri* positions of pentacene was the first functionalization strategy

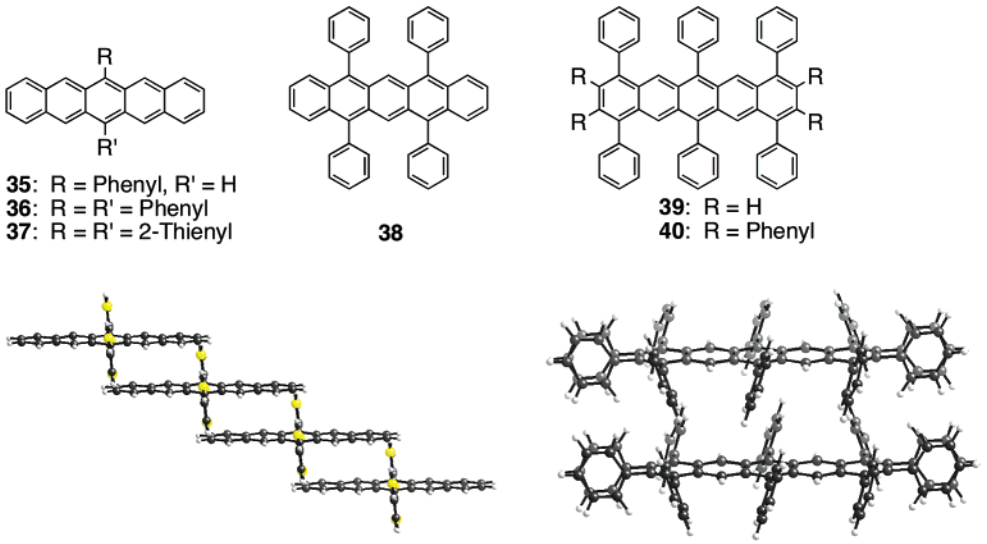

Figure 17. Aryl-functionalized pentacenes studied for hole-transport properties (top) and crystal packing of **37** (bottom left) and **40** (bottom right). Crystallographic data for these compounds are available for download free of charge on the Internet as Supporting Information for ref 71 at http://pubs.acs.org.

Scheme 2. Synthesis of Alkyne-Functionalized Pentacenes with Spherical Solubilizing Groups and the Relationship between Functional Group Diameter and Acene Length

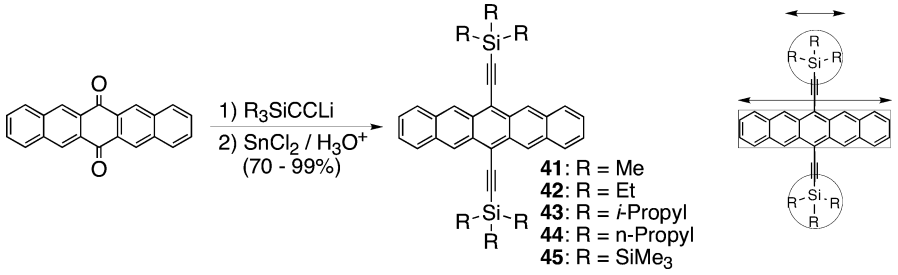

of any sort reported for this molecule.[70] Varying the nature and location of such groups around the pentacene perimeter has recently led to an array of solid-state arrangements (Figure 17), and detailed studies of both thin-film and single-crystal devices performed on this series of molecules elucidated the effect of intermolecular order on charge transport.[71] Although a wide variety of intermolecular arrangements were surveyed as part of this study, only the thienyl derivative **37** exhibited long-range π-stacking order, and consequently it was the only derivative to show high thin-film hole mobility in vapor-deposited films (0.1 cm^2/V s). Perhaps this study's most surprising result arose from the measurement of the hole mobility in transistor devices fabricated on the surface of high-quality single crystals of decaphenyl pentacene **40**. While this material shows no significant close contacts between the acene rings in the crystal (the closest $C_{Ar}-C_{Ar}$ contact is $\sim$5 Å) and thus would not be expected to be an efficient medium for charge transport, single-crystal FET measurements showed a hole mobility of 0.0014 cm^2/(V s). This remarkable finding clearly underscores the importance of single-crystal measurements to the understanding of charge transport in aromatic crystals, as well as the benefit of systematic structure−property studies of functionalized acenes.

4.1.3. Alkyne-Functionalized Pentacenes for Organic Transistors

An alternative to adding property-modifying substituents directly to the aromatic ring of an acene is to hold them from the ring by a rigid, sterically undemanding spacer, such as an alkyne (Scheme 2). In this case, altering the size of the substituent on the alkyne provides excellent control over the π-stacking order seen in the crystal.[72]

For roughly spherical substituents (e.g. *tert*-butyl, trialkylsilyl), a substituent diameter less than half the length of the acene leads to a 1-D, "slipped-stack" arrangement (Figure 18, **42**). For a substituent diameter very close to half the length of the acene, the material adopts a 2-D "bricklayer" arrangement (Figure 18, **43**). If the substituent size is increased further, the packing reverts to the slipped-stack arrangement (Figure 18, **44**). As the substituent size is increased further, edge-to-face interactions between the substituent and the aromatic chromophore begin to dominate (as the volume of the substituent is able to completely cover the aromatic surface), and the herringbone arrangement becomes the preferred solid-state arrangement (Figure 18, **45**).[73]

Device performance of these materials in thin-film FETs is clearly related to the crystal packing arrangements adopted by the molecules. Of all the functionalized pentacene materials in this class studied to-date, *only* those that exhibit 2-D π-stacking interactions yield high-performance thin-film devices.[74] In the case of thermally evaporated film FETs, the highest mobility found for a 1-D π-stacked material (e.g. derivative **42**) was less than 0.001 cm^2/(V s). In contrast the triisopropyl silyl (TIPS) derivative **43**, which packs with strong two-dimensional face-to-face interactions, yielded evaporated film devices with excellent hole mobility (0.4 cm^2/(V s)) when deposited under similar conditions. Further optimization of vapor deposited films of TIPS pentacene **43**

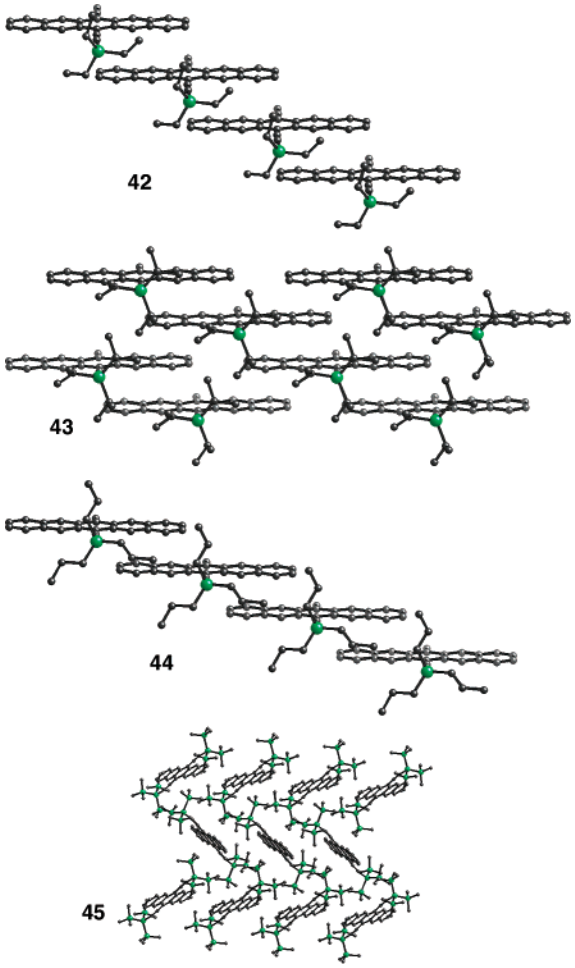

Figure 18. The progression of crystal packing induced by increasing substituent size, from 1-D π-stack (**42**) to 2-D π-stack (**43**) to 1-D π-stack (**44**) to herringbone (**45**). Some silyl groups omitted for clarity. See CSD RefCodes CADMOK and VOQBIM.

is hindered by a relatively low-temperature phase transition that leads to cracking of the crystals and crystalline films of the material (which precludes thermal annealing of the films)[75] and by the narrow substrate temperature range (85−90 °C) under which crystalline films will grow. These issues arise due to thermal rearrangements of the alkyl groups that give the material both solubility and desirable packing.

Solution deposition of **43** yields much higher quality films, since slow evaporation of the solvent allows the materials to self-assemble into large π-stacked arrays. Spin-casting is the most common method used to make uniform thin films of soluble organic molecules but is the method least likely to yield highly crystalline films of **43** due to the speed with which the solvent evaporates. Even so, spin-cast films of **43** yield FET devices with hole mobility as high as 0.2 $cm^2/(V\ s)$ and on/off current ratios of 10^6. A better method for crystalline film formation is drop-casting, where a 1 wt % solution of **43** dissolved in toluene is deposited on top of a bottom-contact FET device substrate, and the solvent is allowed to evaporate slowly. Films formed under these conditions show molecular step terracing when analyzed by atomic force microscopy, signifying a high degree of order in the film. Hole mobilities greater than 1.8 $cm^2/(V\ s)$ and on/off current ratios of 10^8 have been achieved from this deposition method.[76] These values compare well with typical values observed for devices fabricated from vapor-deposited pentacene and are competitive with devices made from amorphous silicon, the current semiconductor used in active matrix displays. While drop-casting is not suitable for large-area deposition, it is the technique most similar to inkjet printing, a process predicted to yield the low-cost devices predicted for organic electronics.[77]

Carrier mobility in single crystals and thin films of pentacene (**32**), TIPS-substituted pentacene **43** and triethylsilyl-substituted pentacene **42** were all investigated using time-resolved terahertz pulse spectroscopy,[78] a contactless method for comparing carrier mobility between organic solids. These experiments confirmed the strong correlation between thin-film morphology and hole mobility for compound **43**, and single-crystal experiments suggested that the hole mobilities for TIPS-pentacene **43** and unsubstituted pentacene **32** should be quite similar.[79] In contrast to the thin-film device measurements, which showed a difference in hole mobility for 2-D π-stacked **43** and 1-D π-stacked **42** of over a factor of 1000, this technique yielded a hole mobility for **42** that was only a factor of 3 smaller than that measured for **43**.[80] Here again, the lower quality films formed by materials that exhibit one-dimensional π-stacking interactions lead to significant underestimates of the intrinsic carrier mobilities of these compounds.

Functionalized pentacene **43** has also been deposited from solution as the first layer in a pentacene/C_{60} photovoltaic device. Careful optimization of deposition conditions, the concentration of mobile ion dopants, thermal postfabrication annealing, and the addition of an exciton-blocking layer yielded a device with a white-light power conversion efficiency of 0.52%.[81] Further improvement in efficiency will require careful optimization of the p-type material's absorption cross-section and HOMO energy level, while the possibility of fully solution-processed small-molecule solar cells will require the development of compatible, soluble

Scheme 3. Synthesis of Partially Fluorinated Derivatives 46 and 47

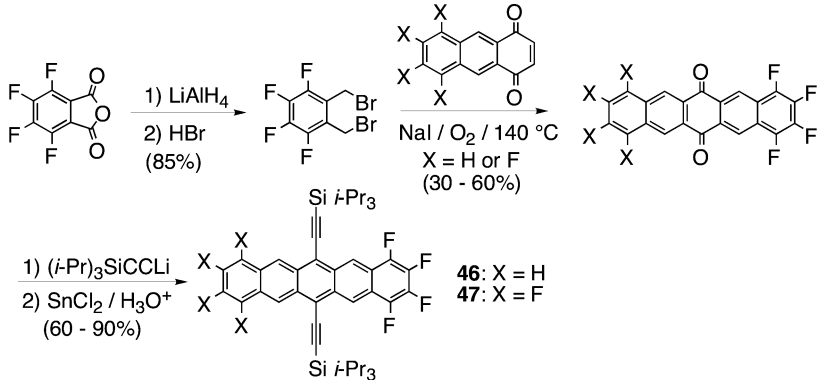

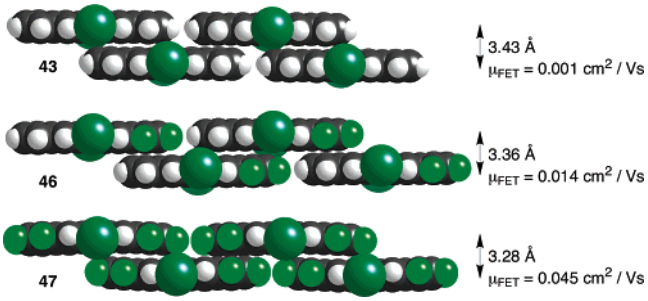

Figure 19. Changes in crystal packing of TIPS pentacene derivatives due to aryl−fluoroaryl interactions and their effect on hole mobility. Crystallographic data for these compounds can be downloaded free from the Internet as Supporting Information for ref 82 at http://pubs.acs.org.

n-type organic semiconductors.

4.1.4. Alkyne-Functionalized Fluoropentacenes

In an attempt to decrease interplanar spacing of the silylethynyl pentacene units in the crystal, two partially fluorinated derivatives of **43** (**46**, **47**) were prepared, as outlined in Scheme 3.[82]

The overall packing arrangement of these fluorinated species is not significantly different from that of **43**, except that the spacing between π-faces decreases with increasing fluorine content, from 3.43 Å for nonfluorinated **43** to 3.28 Å for octafluoro compound **47** (Figure 19). Because each of these derivatives required significantly different conditions for optimum film formation (especially because **39** was not sufficiently soluble to allow deposition by solution methods), FET devices were formed by evaporating films of these materials under identical conditions onto unheated substrates. Even so, the difference in hole mobility among these three derivatives is significant and increases with increasing fluorine content (Figure 19). As with the tetracene derivatives reported by Swager and co-workers, the addition of fluorine substituents is a simple method to control the interplanar spacing of acenes for electronics applications.

4.1.5. Alkyne-Functionalized Alkyl and Alkynyl Pentacenes

To further improve the device characteristics of silylethynyl-substituted pentacenes, additional functionalization was explored to lower the oxidation potential and facilitate charge injection into the organic layer. Initially, alkyl groups were added to the pentacene chromophore (building on the work by Wudl and co-workers on tetramethyl pentacene) (Figure 20). While the addition of alkyl groups did significantly decrease the oxidation potential (0.7 V for methyl derivative **48**, 0.69 V for octyl derivative **49**, compared with 0.85 V for TIPS-pentacene **43,** all values vs standard calomel electrode (SCE)), the crystallinity was significantly perturbed. In the best case (**48**), the packing changed to yield only 1-D face-to-face interactions in the crystal.[83] In the worst (**49**), crystals could not be grown, and X-ray diffraction analysis of spin-cast or drop-cast films showed no evidence of crystallinity.

Recently, Neckers and co-workers reported a series of more highly ethynylated pentacene derivatives (**50**), where the alkyne substituents were used to tune the redox potentials of the pentacene.[84] While no crystallographic analyses or device data were presented for this series of compounds, thin-film UV−vis spectra did show some degree of electronic interaction in the solid state, indicated by measurable (up to

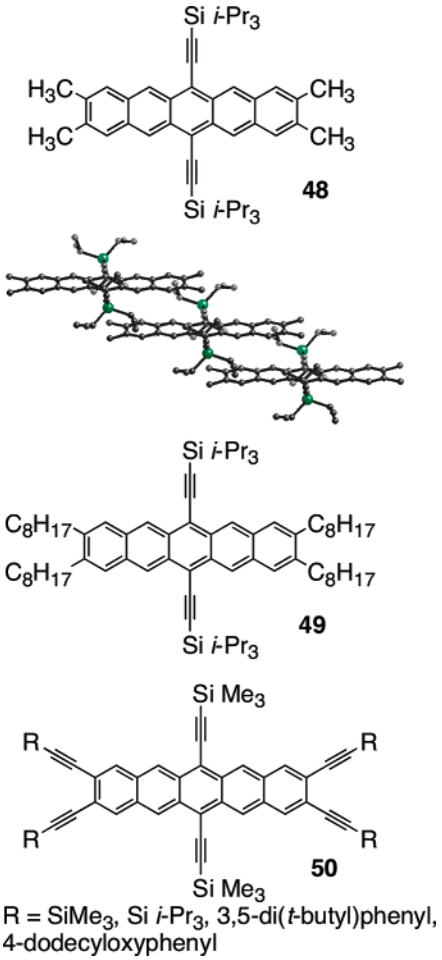

Figure 20. Alkyl-substituted pentacene derivatives **48**−**50** and the crystalline order of compound **48**, showing 1-D π-stacking interactions.

70 nm) red shift in absorption in thin films of the materials compared with their solution absorption maxima.

4.1.6. Alkyne-Functionalized Pentacene Ethers

In an attempt to harness the strong π-electron-donating properties of oxygen substituents to improve hole injection into the pentacene layer of a device, ether functional groups were introduced to the solubilized pentacene chromophore (Figure 21).[85] While acyclic tetraalkoxy TIPS pentacene derivatives were so unstable they could not be isolated, the cyclic dioxane-functionalized pentacene **51** was quite stable, exhibiting the expected red shift in its absorption spectrum and significant decrease in oxidation potential.

The axial hydrogens on the dioxane substituents of **51** were found to inhibit π-stacking of this compound, leading to the synthesis of dioxolane-substituted systems (**52**) to circumvent this issue. Compound **52** indeed crystallizes with significant face-to-face interactions in the solid and has an oxidation potential significantly lower than that of TIPS pentacene **43** (0.69 V vs SCE). The UV−vis spectrum for **52** shows an unusual *blue* shift in absorption (Figure 22), and quite apparent to the eye is also a significant increase in fluorescence quantum yield; solutions of **52** are not the typical "pentacene blue", but rather the solutions are bright red, due to intense emission from this pentacene derivative at 625 nm. This observation led to the use of these dioxolane-based materials in red-emitting OLEDs (see below).

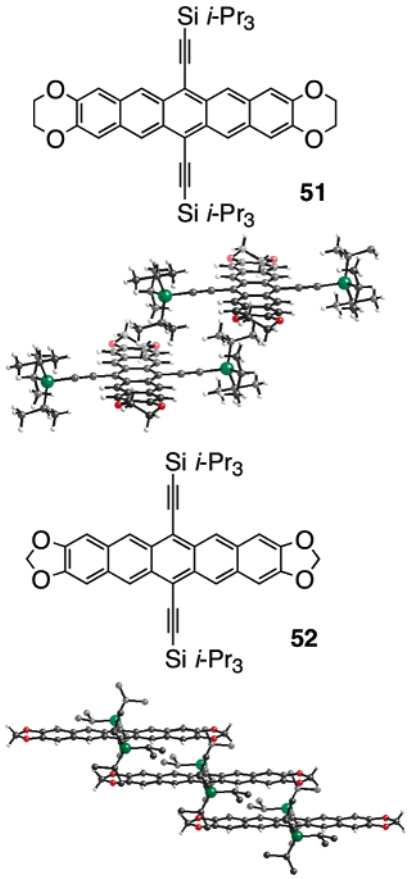

Figure 21. Pentacene ethers **51** and **52** and their crystal packing. Crystallographic data for these compounds are available for download free of charge from the Internet as Supporting Information for ref 85 at http://pubs.acs.org.

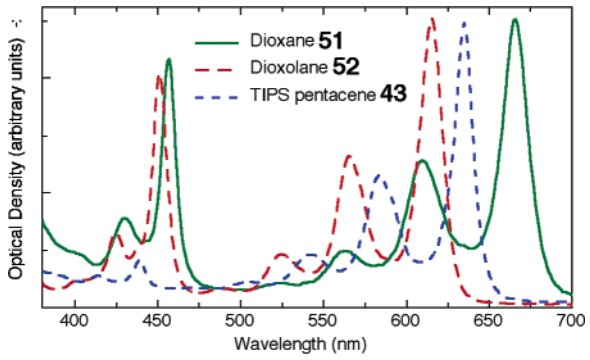

Figure 22. Absorption spectra of pentacene **43** and pentacene ethers **51** and **52**.

Pentacene ether **52** with a triisopropylsilyl-substituted alkyne crystallizes in a 1-D π-stacking arrangement due to the effective lengthening of the chromophore by addition of the rigid dioxolane substituents. Altering this arrangement to yield the more desirable 2-D π-stacking motif required the use of a larger functional group on the alkyne, which was accomplished using the slightly bulkier tri(*n*-propylsilyl) group (**53**).[86] The resulting derivative exhibited the requisite two-dimensional stacking with excellent π-overlap and a closest $C_{Ar}-C_{Ar}$ distance between stacked molecules of 3.40 Å (Figure 23). Unfortunately, attempts to use **53** in a FET device were not successful due to the molecule's propensity to include solvent when crystallizing, leading to poor quality films.

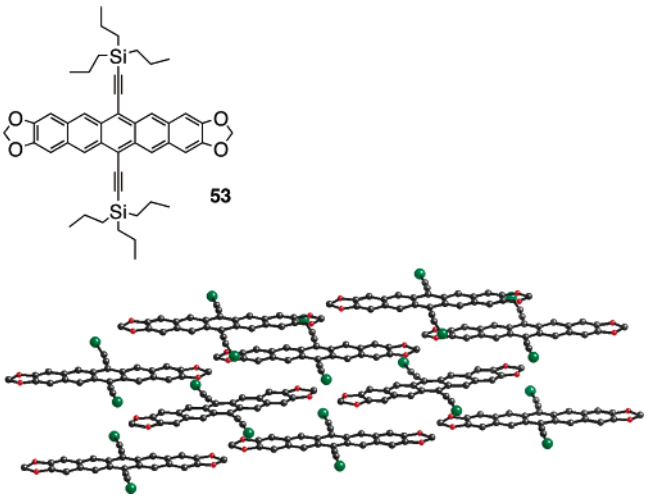

Figure 23. Compound **53** is induced to form 2-D π-stacks (bottom) by carefully adjusting the size of the alkyne substituent (alkyl groups on Si omitted for clarity).

Chart 7

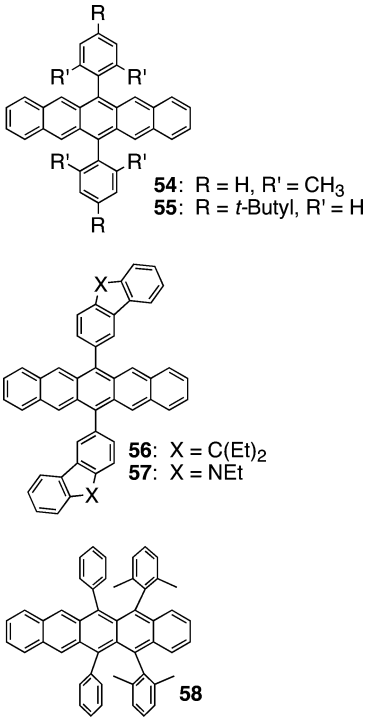

4.2. Functionalized Pentacene Organic Light-Emitting Diodes (OLEDs)

4.2.1. Aryl-Substituted Pentacene

Aryl substitution at the 6,13-positions of pentacene to yield diphenyl pentacene **35** was one of the first functionalization routes investigated to yield amorphous solids for use in red-emitting OLEDs.[87] The promising results presented in the studies of **35** led to the synthesis and study of a broad array of aryl-substituted pentacenes for this purpose (Chart 7). These materials are surprisingly soluble compared with unsubstituted pentacene, to the point of allowing purification by chromatography on silica gel. The aryl derivatives in Chart 7 all show good fluorescence energy transfer from tris-(quinolin-8-olato)aluminum (III) (Alq_3), with pentacene concentrations as low as 0.4 mol % exhibiting excellent red emission with little contribution to emission from the Alq_3

host. While compounds **56** and **57** exhibited relatively low device efficiencies (which the authors attributed to morphological issues created by the large pendant aromatic groups),[88] most of the simple diaryl[89] and tetraaryl[90] derivatives formed devices with reasonable efficiencies. The best external electroluminescence quantum efficiency for red emission was found for compound **55** (1.4% efficiency as a 0.47 mol % dopant in Alq_3), an efficiency close to the theoretical maximum.

4.2.2. Alkyne-Substituted Pentacene Ethers

The absorption profile of dioxolane compound **52** (Figure 22) shows that the wavelengths of light absorbed by this material correspond well to the wavelengths of light emitted by both Alq_3 and 4,4-bis[*N*-1-naphthyl-*N*-phenyl-amino]-biphenyl (NPD, a common hole-transport material used in OLEDs). Extensive studies using **52** as a guest emitter in both Alq_3 and NPD host matrices showed efficient energy transfer and bright red emission for very low concentrations of **52** (less than 0.5 mol %).[91] The appearance of aggregate emissions at higher concentrations of **52** led to the synthesis of a new dioxolane-based derivative functionalized with ethyl groups on the dioxolane ring, designed to increase the separation of π-surfaces in the crystal. Crystallographic analysis of the resulting compound (**59**, Figure 24) showed

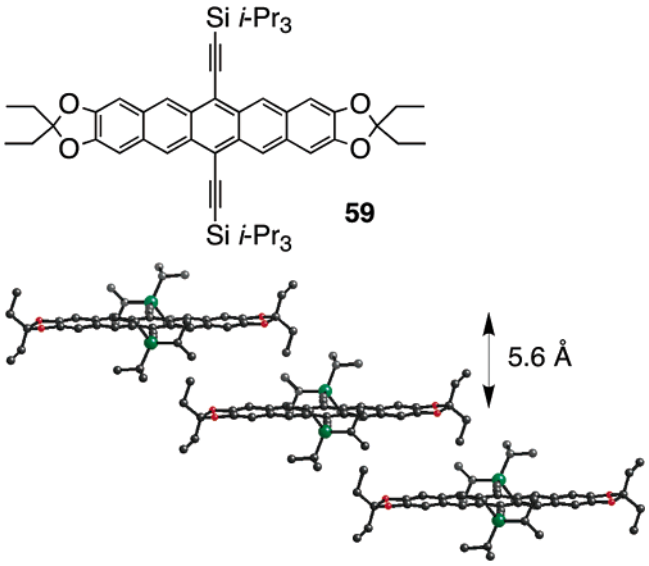

Figure 24. The ethyl substituents on pentacene **59** prevent interactions between aromatic carbon atoms on adjacent molecules. Crystallographic data for this compound are available for download as the Supporting Information for ref 91 at http://pubs.acs.org.

that while the pentacene units are still coplanar, the ethyl groups do indeed act as efficient spacers, preventing significant interactions between the π-surfaces. The nearest $C_{Ar}-C_{Ar}$ contact between adjacent molecules of **59** is more than 5.5 Å. Composite films of **59** with both Alq_3 and NPD as host show bright red emission at all guest concentrations measured (up to 2 mol % guest), and an Alq_3 host/**59** guest OLED device yielded bright red emission with an external electroluminescence quantum yield of 3.3%,[92] very close to the theoretical maximum and also very close to the best value reported (3.6%[93]) for a small-molecule red-emissive OLED.

Chart 8

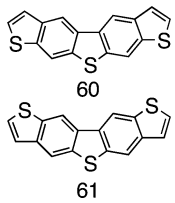

4.3. Heteropentacenes for Organic Transistors

4.3.1. Thieno Bis(benzothiophene)s

Neckers and co-workers recently reported an isomer-specific synthesis of two thieno bis(benzothiophenes) (Chart 8), along with thorough characterization of these materials.[94] Crystallographic analysis of compound **61** showed that the molecules crystallize in a coplanar arrangement and yield uniform surface coverage when deposited on SiO_2 by thermal evaporation under vacuum. FET mobilities for **60** and **61** are 0.011 and 0.12 $cm^2/(V\ s)$, respectively. This difference of an order of magnitude in mobility between two very similar isomers is likely due to the difference in grain sizes observed by the authors upon AFM analysis of the thin films, with large grains and poorer surface coverage noted for **60**.

4.3.2. Anthradithiophene and Dialkylanthradithiophenes

One of the most thoroughly studied heteropentacenes is anthradithiophene (ADT), which was prepared as part of an early effort to discover new materials for organic transistors by Katz and co-workers.[95] The relatively straightforward synthesis of this compound begins with anthradithioiphene-quinone, formed as an inseparable mixture of isomers from the condensation of thiophene-2,3-dicarboxaldehyde with 1,4-cyclohexanedione.[96] This mixture of quinones is easily reduced to the corresponding heteropentacenes (Scheme 4). While evaporated films of the parent ADT **62** only yield moderate mobility in a FET device (0.09 $cm^2/(V\ s)$), just as with oligothiophenes[97] the thiophene units of ADT can be substituted with alkyl chains that dramatically improve film quality. The dihexyl and didodecyl derivatives **63** and **64** both yielded evaporated films of significantly improved

Scheme 4. Synthesis of Anthradithiophene 62 and 2,8-Dialkyl Anthradithiophenes 63−65

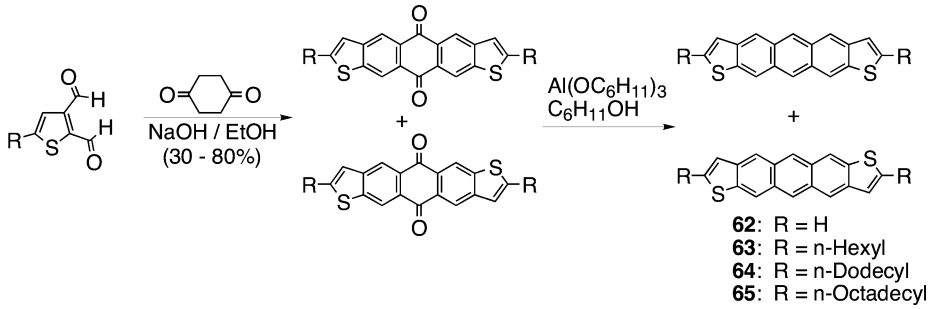

quality and formed transistors with carrier mobilities of 0.15 $cm^2/(V\ s)$. More importantly, the alkyl-substituted materials were sufficiently soluble to allow film formation by solution casting, resulting in devices with mobilities of 0.02 $cm^2/(V\ s)$ (a similar solution deposition attempt was made with unsubstituted pentacene but was unsuccessful due to the rapid photobleaching of the pentacene solution).[98] These ADT derivatives constituted one of the first demonstrations of solution-cast small molecules not requiring high-temperature annealing to achieve measurable mobility.

4.3.3. Alkyne-Functionalized Anthradithiophenes

Analogous to the previously reported pentacene functionalization approach, a strategy involving silylethyne substitution was also applied to anthradithiophene (Scheme 5).

Scheme 5. Synthesis of Silylethynyl-Functionalized Anthradithiophenes 66−68

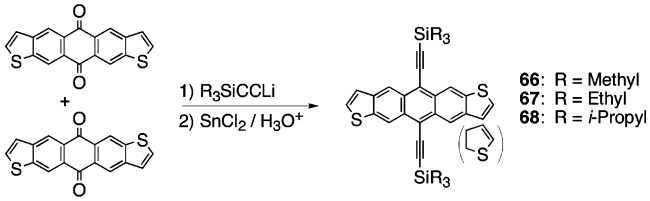

Starting with the same *syn*- and *anti*-anthradithiophenequinone mixture used by Katz and co-workers, a variety of trialkylsilyl acetylenes were appended to the anthradithiophene core to yield several solid-state arrangements with small changes in the size of the alkyne substituent leading to significant changes in the crystalline order.[99]

The trimethylsilyl derivative **66** exhibits primarily edge-to-face interactions in the crystal, both between the silyl group and the aromatic face and between the terminal thiophene position and the aromatic face of an adjacent molecule (Figure 25). The triethylsilyl derivative **67** adopts

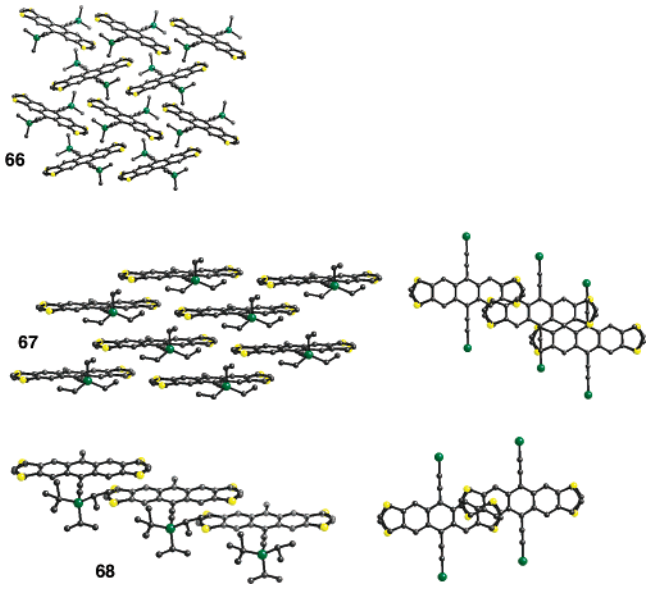

Figure 25. Crystalline order of anthradithiophenes **66**−**68** (some trialkylsilyl groups omitted for clarity). Views normal to the aromatic plane for **67** and **68** show details of π-overlap with nearest neighbor molecule(s) (CSD RefCodes MAMNUK, MAMPAS, and FANGUX).

a 2-D π-stacking motif very similar to TIPS-pentacene **43**, while the triisopropylsilyl derivative **68** adopts a 1-D, slipped-stack arrangement similar to pentacene derivative **42**. These unique crystalline arrangements of essentially identical chromophores lead to radically different appearances of the crystals; the trimethylsilyl derivative produces red/pink needles, the triethylsilyl derivative produces deep purple plates, and the triisopropylsilyl derivative produces tiny, bright orange cubes.

Analysis of solution-deposited films of **66**−**68** in a bottom-contact field-effect transistor configuration further supported the strong correlation between crystalline order and device performance. Both the edge-to-face interacting **66** and the 1-D slipped-stacked **68** showed relatively poor device performance, with hole mobility only as high as 0.05 $cm^2/(V\ s)$ for **68**. However, drop-cast films of **67** yielded devices with mobilities as high as 1.0 $cm^2/(V\ s)$ and on/off current ratios of 10^7, both parameters well within the range necessary for useful commercial devices. It should be noted that **67** did suffer from significant barriers to charge injection from the electrodes, most likely due to its very high oxidation potential (0.91 V vs SCE). In this case, the high oxidation potential and larger HOMO−LUMO gap did not improve the photostability of this material; thin films of **67** photobleach within minutes, requiring all measurements to be taken in the dark.

4.3.4. Pentathienopentacene

In an approach designed to replace all of the carbocyclic rings of pentacene with heterocyclic systems, Zhu and co-workers reported the synthesis and device study of the linearly fused pentathienoacene **69** (Chart 9).[100] X-ray

Chart 9

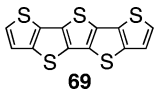

crystallographic analysis of this same compound performed by the Matzger group[101] showed the molecules arranged in the crystal in a coplanar fashion; however, the planes of the carbon backbone of these molecules were separated by a distance (3.88 Å) well outside the optimum separation (3.4 Å) typically preferred for strong electronic interactions.[102] These weak interactions are somewhat mitigated by several close sulfur−sulfur contacts (3.55 Å). Analysis of evaporated films of this compound show that the molecules arrange with their long axes perpendicular to the substrate and appear to adopt in the thin films the same arrangement measured in the single crystals. As a likely result of the significant π-face separation between molecules in the crystals and films, hole mobility measured in FET devices made from **69** were low, with the best films yielding $\mu = 0.045\ cm^2/(V\ s)$.

4.3.5. Azapentacenes

Surprisingly few nitrogen-containing heteropentacenes have been reported,[103] few have been fully characterized structurally, and fewer still have been characterized in electronic devices. Most of these compounds (Chart 10) have shown relatively low mobility, although recent results for transistors fabricated on *amorphous* films of heteropentacenes **70** showed surprisingly high hole mobility (0.02 $cm^2/(V\ s)$) and good device stability.[104] Nuckolls and co-workers recently performed a detailed study of the diazadihydro pentacenes **71**−**73** (among other derivatives).[105] These materials are easily synthesized and purified and are readily

Chart 10

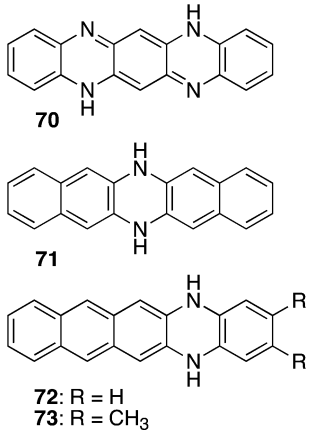

crystallized from solution. Crystals of compound **71** were subjected to X-ray crystallographic analysis, and the molecules were found to arrange in a herringbone fashion similar to pentacene. Vapor-deposited films of these molecules were used in a top-contact device configuration and yielded hole mobilities of 5×10^{-5} cm^2/(V s) for **71** and as high as 6×10^{-3} cm^2/(V s) for **72**. In both cases, on/off current ratio was ~1000. While these mobility values are not high, the materials were reported to be quite stable, and the simplicity of the synthesis of these compounds gives hope that further functionalization may lead to higher-performance materials or for materials for sensing applications.

4.3.6. Carbazole-Based Systems

Pyrrole, like thiophene, can be used in place of some of the aromatic rings of pentacene to yield new heteropentacene materials. A benefit of the nitrogen heteroatom is the open valence available for the addition of further functional groups that can extend conjugation or modify solubility. Ong and co-workers have reported a series of N-alkyl carbazoles, **74**−**76** (Chart 11) that were environmentally stable and whose

Chart 11

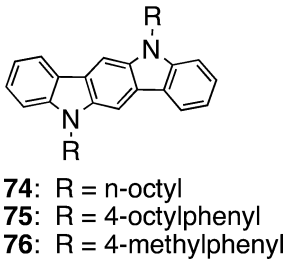

films exhibited mobilities as high as 0.12 cm^2/(V s) (for compound **75**).[106] The exact nature of the nitrogen substituent was shown to be critical, and the only materials exhibiting promising device performance contained groups that both extended conjugation (aryl rings) and contained alkyl groups to direct the molecules' self-assembly. The authors explored the effect of further functionalization of these systems by the addition of halogen groups to the aryl rings of the aromatic core, but these additions did not improve device performance.[107]

5. Higher Heteroacenes

Fused aromatic compounds with more than five rings pose a daunting synthetic challenge,[108] and their usual low stability

Chart 12

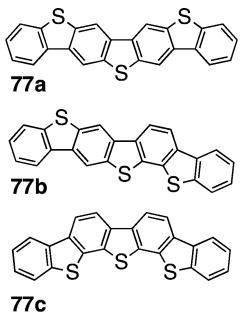

and poor solubility further impede their preparation, characterization, and device study. Fortunately, larger heteroacenes do not suffer from these complications to such an extent. Thus, one of the earliest reported high-performance organic semiconductors was a seven-ringed dibenzothieno bisbenzothiophene (**77**, Chart 12), prepared as a mixture of three isomers that could not be separated by normal chemical means.[109] However, careful sublimation of this compound during device fabrication, keeping the shutter protecting the device substrate closed until most of the material in the evaporation boat had been sublimed, led to the deposition of mostly **77a** from the mixture. Devices made in this fashion had hole mobility of 0.15 cm^2/(V s); without this careful control of sublimation conditions, the mixture of isomers is deposited, leading to low film quality and hole mobility of less than 0.03 cm^2/(V s). The significant difference in geometry of the three isomers of **77** likely leads to different crystal packing arrangements for the molecules, and deposition of the mixture of species would thus yield films with poor morphologies for device applications.

5.1. Larger Heteroacenes as Models for Higher Acenes

The higher oxidation potential and larger HOMO−LUMO gap per aromatic ring of the heteroacenes vs the carbocyclic acenes make the former class of compounds ideal candidates for exploring the chemistry of larger acenes. While heptacene **78** (Chart 13) has remained an elusive compound (both in

Chart 13

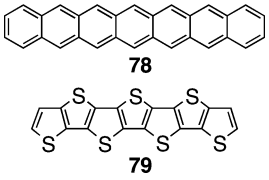

its synthesis and in understanding its likely properties),[110] heptathienoacene **79**, for example, is very stable, and solubilized versions can be easily isolated and characterized.[111] Increasing the proportion of carbocyclic rings in compounds such as **79** will allow an approximation of the properties of the fully carbocyclic higher acenes and will yield insight into functionality required to stabilize these reactive systems.

5.1.1. Higher Acenedithiophenes

Acenedithiophenes are attractive targets as models of higher acenes because of the unperturbed acene core present in these systems: increasing the length of acenedithiophene requires increasing the length of this acene core, leading to

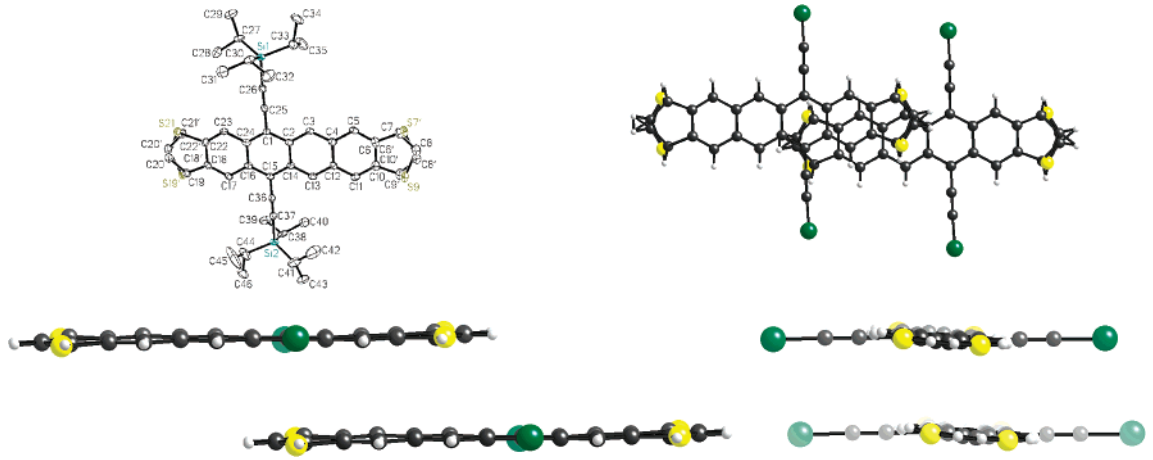

Figure 26. Structure and crystallographic packing of functionalized tetradithiophene **80**, showing degree of π-face overlap (alkyl groups on Si removed for clarity) (CSD RefCode FANHAE).

Scheme 6. Synthesis of Six-Ringed and Seven-Ringed Heteroacenes 80−82

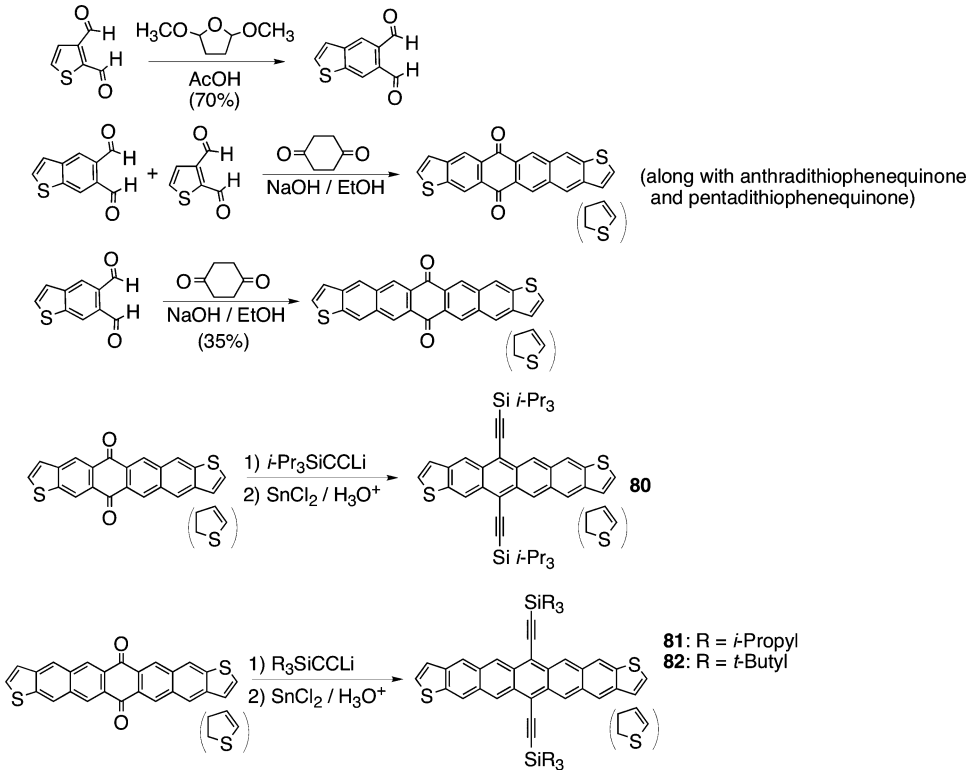

a rapid evolution of electronic properties. Acenedithiophenes with five linearly-fused rings are also a proven class of organic semiconductor, which adds additional motivation to the study of higher homologues of this system.

Using a well-known homologation reaction on thiophene 2,3-dicarboxaldehyde (Scheme 6),[112] the *syn*- and *anti*-mixtures of tetradithiophene and pentadithiophene quinones were prepared in a straightforward manner. Application of a simple ethynylation strategy led to soluble heteroacenes containing six and seven linearly fused rings.[113]

The tetradithiophene **80** was isolated by chromatography on silica gel (to remove **81** and **68** that also formed in the reaction) as a blue crystalline solid. The material was relatively soluble in halogenated or aromatic solvents, was environmentally stable, and had an oxidation potential of 0.72 V (vs SCE). Crystallographic analysis (Figure 26) showed that the material adopted a 1-D π-stacked order in the solid (as would be expected comparing the diameter of the Si group to the length of the acene).

Analysis of the heteroheptacene derivative **81** proved difficult; NMR spectroscopic characterization showed significantly less symmetry than was expected for such a simple molecule. X-ray crystallographic analysis of the green crystals revealed that the material isolated was actually the product of a Diels−Alder reaction between one heteroheptacene ring and the alkyne of another substituted heteroheptacene (Figure 27).

Because **81** still contained an intact heteroheptacene ring system, it was postulated that a stable heteroheptacene could be isolated by simply preventing the Diels−Alder side reaction. By an increase of the size of the alkyne substituent to tri(*tert*-butylsilyl), the dienophile capability of the alkyne was sufficiently reduced[114] that derivative **82** could be isolated as a green solid that was stable and soluble enough

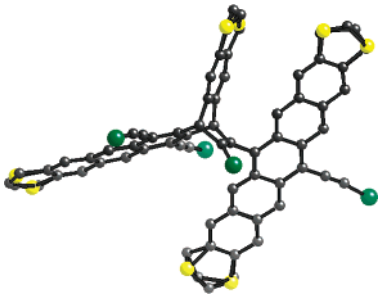

Figure 27. Diels−Alder dimer of pentadithiophene **81** (alkyl groups on Si omitted for clarity) (CSD RefCode FANGOR).

to be fully characterized. Compound **82** has $\lambda_{max} = 762$ nm and an oxidation potential of 0.61 V vs SCE. Crystals grown from CS_2 were subjected to crystallographic analysis, which both confirmed the structure and revealed that this large heteroacene adopts a familiar 1-D slipped-stack arrangement in the solid state (Figure 28).

The performance of tetradithiophene **80** in field-effect transistors was poor ($\mu = 3 \times 10^{-5}$), due to poor surface coverage by the solution-deposited film (likely because this derivative adopts a one-dimensional π-stacked arrangement in the crystal).[115] Despite the low thin-film mobility, this compound has been used as the electron-donating layer of an all solution-deposited solar cell (with the fullerene derivative PCBM as the electron-accepting layer),[116] which is only possible because of the extremely slow reaction between acenedithiophenes and fullerenes.[117] The use of pentadithiophene **82** in organic electronic devices was hampered by it slow solubility and poor film stability.

5.2. Higher Acenes: Functionalized Hexacenes and Heptacenes

The study of the larger acenedithiophenes shed significant light on the parameters required for the successful functionalization of higher acenes. When it was observed that the ethynylation of hexacenequinone with triisopropylsilyl acetylene led to a fleetingly stable derivative, it was assumed that a Diels−Alder reaction similar to that seen in pentadithiophene **81** was occurring, leading to the adoption of the

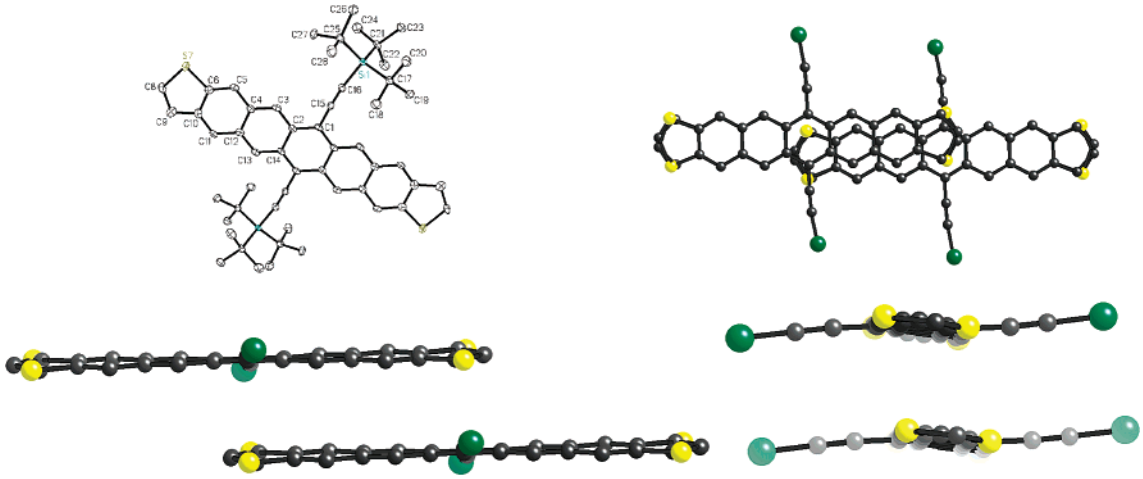

Figure 28. Structure and crystallographic packing of functionalized pentadithiophene **82**, showing degree of π-face overlap (alkyl groups on Si removed for clarity) (CSD RefCode FANGIL).

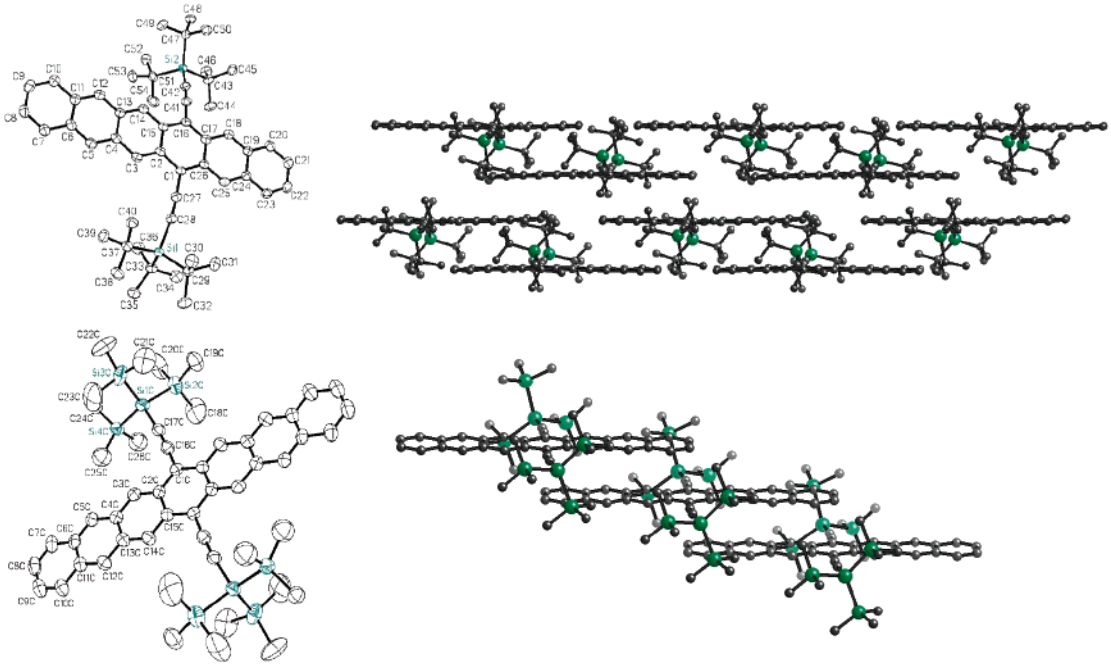

Figure 29. Structure and crystal packing of hexacene **84** (top) and heptacene **86** (bottom). Crystallographic data for these compounds are available for download free of charge as the Supporting Information for ref 118 at http://pubs.acs.org.

Scheme 7. Synthesis of Functionalized Hexacene and Heptacene

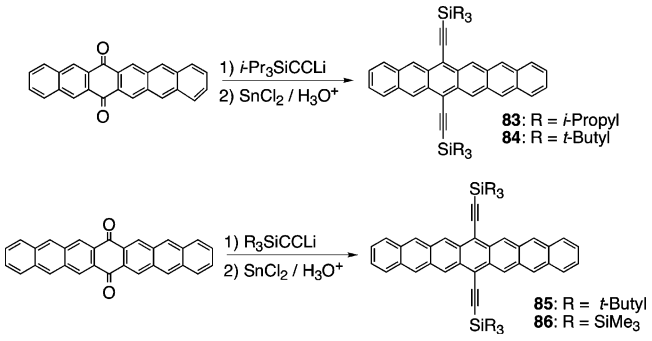

bulkier tri(*tert*-butylsilyl) group for the synthesis of **84** (Scheme 7).[118] Hexacene **84** is a stable, soluble, easily chromatographed deep green material that crystallizes readily from toluene. This derivative of hexacene is stable for >1 year in the crystalline state and for several weeks in solution provided air and light are excluded. Hexacene **84** has an oxidation potential of 0.66 V (vs SCE), yielding a better match with the work function of gold electrodes than the silylethyne-functionalized pentacene derivatives such as **43**. Crystallographic analysis (Figure 29) shows that **84** possesses an essentially planar aromatic backbone (although the alkynes are severely distorted from the packing) and that the molecule adopts a 2-D π-stacked arrangement similar to TIPS-pentacene **43**, an arrangement shown to be very favorable for the fabrication of high-mobility devices.

The isolation of a characterizable heptacene derivative required the use of an even bulkier substituent on the alkyne. Even with the extraordinarily bulky tris(trimethylsilyl)silyl group pendant to the heptacene framework, **86** is only stable in the crystalline state for a period of a few weeks. Heptacene **86** was sufficiently soluble for complete characterization by proton and carbon NMR spectroscopy, as well as UV−vis spectroscopy and cyclic voltammetry (showing an oxidation potential of 0.47 V vs SCE and λ_{max} of 855 nm). The pale yellow-green crystals of **86** were subjected to X-ray crystallographic analysis, which along with confirming the heptacene structure, showed a planar aromatic backbone adopting a 1-D π-stacking arrangement (Figure 29).

6. Conclusions

For applications involving charge transport through organic films, precise control of molecular ordering in the solid state is crucial. The ability to functionalize acenes to control the general type of interaction occurring in the crystal (herringbone vs π-stacking) is a critical aspect for improving the performance of organic semiconductors, and detailed structure−property relationship studies described in this review are bringing to light the precise types of interactions most beneficial to device applications. Across a wide variety of derivatives, it was shown that materials with extensive face-to-face interactions generally exhibited hole mobilities superior to those systems with strictly edge-to-face interactions. Furthermore while one-dimensional π-stacking interactions are present in systems with very high single-crystal mobilities (e.g., rubrene), materials with two-dimensional interactions, whether these interactions are of a face-to-face (TIPS-pentacene **43**) or edge-to-face (e.g., pentacene **32**) nature, yield the highest-performance thin-film devices. As the general parameters required for efficient charge transport in organic crystals and films come to light, researchers are beginning to focus on further tuning the properties of these semiconductors to improve other device-critical parameters such as solubility, stability, or interfacial issues, to maximize their performance in devices. New generations of materials exhibit many performance parameters that rival those of traditional, amorphous inorganic semiconductor materials (such as thin-film mobilities in excess of 3 cm^2/Vs), and the near-infinite "tunability" of organic materials is now making them attractive targets for commercial applications.

7. Acknowledgments

We are grateful to the Office of Naval Research and the Defense Advanced Research Projects Agency for their support.

8. References and Notes

(1) (a) Kelley, T. W.; Baude, P. F.; Gerlach, C.; Ender, D. E.; Muyres, D.; Haase, M. A.; Vogel, D. E.; Theiss, S. D. *Chem. Mater.* **2004**, *16*, 4413. (b) Sun, Y.; Liu, Y.; Zhu, D. *J. Mater. Chem.* **2005**, *15*, 53.

(2) For an excellent review on the commercial prospects of organic electronics, see: Sheats, J. R. *J. Mater. Res.* **2004**, *19*, 1974.

(3) See, for example: (a) Gundlach, D. J.; Nichols, J. A.; Zhou, L.; Jackson, T. N. *Appl. Phys. Lett.* **2002**, *80*, 2925. (b) Hepp, A.; von Malm, N.; Schmechel, R.; von Seggern, H. *Synth. Met.* **2003**, *138*, 201.

(4) (a) Müllen, K.; Wegner, G. *Electronic Materials: The Oligomer Approach*; Wiley-VCH: New York, 1998. (b) Faid, K.; Frechette, M.; Ranger, M.; Mazerolle, L.; Levesque, I.; Leclerc, M.; Chen, T.-A.; Rieke, R. D. *Chem. Mater.* **1995**, *7*, 1390.

(5) See, for example: Valdes-Aguilera, O.; Neckers, D. C. *Acc. Chem. Res.* **1989**, *22*, 171.

(6) Kazmaier, P. M.; Hoffmann, R. *J. Am. Chem. Soc.* **1994**, *116*, 9684.

(7) (a) Brédas, J.-L.; Calbers, J. P.; da Silva Filho, D. A.; Cornil, J. *Proc. Nat. Acad. Sci. U.S.A.* **2002**, *99*, 5804. (b) Cornil, J.; Beljonne, D.; Calbert, J. P.; Brédas, J.-L. *Adv. Mater.* **2001**, *13*, 1053. (c) For a review, see: Brédas, J.-L.; Beljonne, D.; Coropceanu, V.; Cornil, J. *Chem. Rev.* **2004**, *104*, 4971.

(8) (a) Cheng, Y. C.; Silbey, R. S.; da Silva Filho, D. A.; Calbert, J. P.; Cornil, J.; Brédas, J. L. *J. Chem. Phys.* **2003**, *118*, 3764. (b) Gruhn, N. E.; da Silva Filho, D. A.; Bill, T. G.; Malagoli, M.; Coropceanu, V.; Kahn, A.; Brédas, J. L. *J. Am. Chem. Soc.* **2002**, *124*, 7918. (c) Coropceanu, V.; Malagoli, M.; da Silva Filho, D. A.; Gruhn, N. E.; Bill, T. G.; Brédas, J. L. *Phys. Rev. Lett.* **2002**, *89*, No. 275503. (d) Cornil, J.; Calbert, J. Ph.; Brédas, J. L. *J. Am. Chem. Soc.* **2001**, *123*, 1250. For similar studies on functionalized pentacene, see: (e) Troisi, A.; Orlandi, G.; Anthony, J. E. *Chem. Mater.* **2005**, *17*, 5024. (f) Haddon, R. C.; Chi, X.; Itkis, M. E.; Anthony, J. E.; Eaton, D. L.; Siegrist, T. *J. Phys. Chem. B* **2002**, *106*, 8288.

(9) Kwon, O.; Coropceanu, V.; Gruhn, N. E.; Durivage, J. C.; Laquindanum, J. G.; Katz, H. E.; Cornil, J.; Brédas, J. L. *J. Chem. Phys.* **2004**, *120*, 8186.

(10) For a review, see: Katz, H. E.; Bao, Z. *J. Phys. Chem. B* **2000**, *104*, 671.

(11) Li, X.-C.; Sirringhaus, H.; Garnier, F.; Holmes, A. B.; Moratti, S. C.; Feeder, N.; Clegg, W.; Teat, S. J.; Friend, R. H. *J. Am. Chem. Soc.* **1998**, *120*, 2206.

(12) For an excellent description of solid-state aromatic interactions, see: Curtis, M. D.; Cao, J.; Kampf, J. W. *J. Am. Chem. Soc.* **2004**, *126*, 4318.

(13) Ito, K.; Suzuki, T.; Sakamoto, Y.; Kubota, D.; Inoue, Y.; Sato, F.; Tokito, S. *Angew. Chem., Int. Ed.* **2003**, *42*, 1159.

(14) Ando, S.; Nishida, J.-I.; Fujiwara, E.; Tada, H.; Inoue, Y.; Tokito, S.; Yamashita, Y. *Chem. Mater.* **2005**, *17*, 1261.

(15) For detailed discussions of the preferred crystalline orientation of a variety of aromatic molecules, see: (a) Sarma, J. A. R. P.; Desiraju, G. R. *Acc. Chem. Res.* **1986**, *19*, 222. (b) Jennings, W. B.; Farrell, B. M.; Malone, J. F. *Acc. Chem. Res.* **2001**, *34*, 885. (c) Desiraju, G. R.; Gavezzotti, A. *Acta Crystallogr.* **1989**, *B45*, 473. (d) Gavezzotti, A.; Desiraju, G. R. *Acta Crystallogr.* **1988**, *B44*, 427.

(16) Meng, H.; Sun, F.; Goldfinger, M. B.; Jaycox, G. D.; Li, Z.; Marshall, W. J.; Blackman, G. S. *J. Am. Chem. Soc.* **2005**, *127*, 2406.

(17) (a) Kim, Y.-H.; Shin, D.-C.; Kim, S.-H.; Ko, C.-H.; Yu, H.-S.; Chae, Y.-S.; Kwon, S.-K. *Adv. Mater.* **2001**, *13*, 1690. (b) Zhang, Z. L.; Jiang, X. Y.; Zhu, W. Q.; Zheng, X. Y.; Wu, Y. Z.; Xu, S. H. *Synth.*

Met. **2003**, *137*, 1141. (c) Zhang, X. H.; Liu, M. W.; Wong, O. Y.; Lee, C. S.; Kwong, H. L.; Lee, S. T.; Wu, S. K. *Chem. Phys. Lett.* **2003**, *369*, 478. (d) Shi, J.; Tang, C. W. *Appl. Phys. Lett.* **2002**, *80*, 3201. (e) Liu, T.-H.; Shen, W.-J.; Yen, C.-K.; Iou, C.-Y.; Chen, H.-H.; Banumathy, B.; Chen, C. H. *Synth. Met.* **2003**, *137*, 1033.

(18) Shi, J.; Tang, C. W. *Appl. Phys. Lett.* **2002**, *80*, 3201.

(19) Duong, H. M.; Bendikov, M.; Steiger, D.; Zhang, Q.; Sonmez, G.; Yamada, J.; Wudl, F. *Org. Lett.* **2003**, *5*, 4433.

(20) Xu, Q.; Duong, H. M.; Wudl, F.; Yang, Y. *Appl. Phys. Lett.* **2004**, *85*, 3357.

(21) Landis, C. A.; Parkin, S. R.; Anthony, J. E. *Jpn. J. Appl. Phys.* **2005**, *44*, 3921.

(22) Laquindanum, J. G.; Katz, H. E.; Lovinger, A. J.; Dodabalapur, A. *Adv. Mater.* **1997**, *8*, 36.

(23) Katz, H. E.; Bao, Z.; Gilat, S. L. *Acc. Chem. Res.* **2001**, *34*, 359.

(24) Takimiya, K.; Kunugi, Y.; Konda, Y.; Niihara, N.; Otsubo, T. *J. Am. Chem. Soc.* **2004**, *126*, 5084.

(25) Li, X.-C.; Sirringhaus, H.; Garnier, F.; Holmes, A. B.; Moratti, S. C.; Feeder, N.; Clegg, W.; Teat, S. J.; Friend, R. H. *J. Am. Chem. Soc.* **1998**, *120*, 2206.

(26) For an excellent model for the quantification of the precise nature of intermolecular overlap, see: Curtis, M. D.; Cao, J.; Kampf, J. W. *J. Am. Chem. Soc.* **2004**, *126*, 4318.

(27) Iosip, M. D.; Destri, S.; Pasini, M.; Porzio, W.; Pernstich, K. P.; Batlogg, B. *Synth. Met.* **2004**, *146*, 251.

(28) Cicoira, F.; Santato, C.; Melucci, M.; Favaretto, L.; Gazzano, M.; Muccini, M.; Barbarella, G. *Adv. Mater.* **2006**, *18*, 169.

(29) (a) Robertson, J. M.; Sinclair, V. C.; Trotter, J. *Acta Crystallogr.* **1961**, *14*, 697. (b) Campbell, R. B.; Robertson, J. M.; Trotter, J. *Acta Crystallogr.* **1962**, *15*, 289 (revision of structure reported in ref 29a). (c) Holmes, D.; Kumaraswamy, S.; Matzger, A. J.; Vollhardt, K. P. C. *Chem.—Eur. J.* **1999**, *5*, 3399.

(30) Reichwagen, J.; Hopf, H.; Del Guerzo, A.; Desvergne, J.-P.; Bouas-Laurent, H. *Org. Lett.* **2004**, *6*, 1899.

(31) (a) Gundlach, D. J.; Nichols, J. A.; Zhou, L.; Jackson, T. N. *Appl. Phys. Lett.* **2002**, *80*, 2925. (b) Cicoira, F.; Santato, C.; Dinelli, F.; Murgia, M.; Loi, M. A.; Biscarini, F.; Zamboni, R.; Heremans, P.; Muccini, M. *Adv. Funct. Mater.* **2005**, *15*, 375. (c) Abthagir, P. S.; Ha, Y.-G.; You, E.-A.; Jeong, S.-H.; Seo, H.-S.; Choi, J.-H. *J. Phys. Chem. B* **2005**, *109*, 23918.

(32) Chu, C.-W.; Shao, Y.; Shrotriya, V.; Yang, Y. *Appl. Phys. Lett.* **2005**, *86*, No. 243506.

(33) (a) Laudise, R. A.; Kloc, C.; Simpkins, P. G.; Siegrist, T. *J. Cryst. Growth* **1998**, *187*, 449. (b) Kloc, C.; Simpkins, P. G.; Siegrist, T.; Laudise, R. A. *J. Cryst. Growth* **1997**, *182*, 416.

(34) Goldmann, G.; Haas, S.; Krellner, C.; Pernstich, K. P.; Gundlach, D. J.; Batlogg, B. *J. Appl. Phys.* **2004**, *96*, 2080.

(35) For a recent review of the progress in the field of transistors fabricated on single-crystal organic surfaces, see: de Boer, R. W. I.; Gershenson, M. E.; Morpurgo, A. F.; Podzorov, V. *Phys. Status Solidi a* **2004**, *201*, 1302.

(36) Sarma, J. A. R. P.; Desiraju, G. R. *Acc. Chem. Res.* **1986**, *19*, 222.

(37) Moon, H.; Zeis, R.; Borkent, E.-J.; Besnard, C.; Lovinger, A. J.; Siegrist, T.; Kloc, C.; Bao, Z. *J. Am. Chem. Soc.* **2004**, *126*, 15322.

(38) Miao, Q.; Lefenfeld, M.; Nguyen, T.-Q.; Siegrist, T.; Kloc, C.; Nuckolls, C. *Adv. Mater.* **2005**, *17*, 407.

(39) Tulevski, G. S.; Miao, Q.; Fukuto, M.; Abram, R.; Ocko, B.; Pindak, R.; Steigerwald, M. L.; Kagan, C. R.; Nuckolls, C. *J. Am. Chem. Soc.* **2004**, *126*, 15048.

(40) Merlo, J. A.; Newman, C. R.; Gerlach, C. P.; Kelley, T. W.; Muyres, D. V.; Fritz, S. E.; Toney, M. F.; Frisbie, C. D. *J. Am. Chem. Soc.* **2005**, *127*, 3997.

(41) For a recent review, see: de Boer, R. W. I.; Gershenson, M. E.; Morpurgo, A. F.; Podzorov, V. *Phys. Status Solidi a* **2004**, *201*, 1302.

(42) Da Silva Filho, D. A.; Kim, E. G.; Brédas, J. L. *Adv. Mater.* **2005**, *17*, 1072.

(43) (a) Podzorov, V.; Menard, E.; Borissov, A.; Kiryukhin, V.; Rogers, J. A.; Gershenson, M. E. *Phys. Rev. Lett.* **2004**, *93*, No. 086602. (b) Menard, E.; Podzorov, V.; Hur, S.-H.; Gaur, A.; Gershenson, M. E.; Rogers, J. A. *Adv. Mater.* **2004**, *16*, 2097.

(44) Podzorov, V.; Menard, E.; Rogers, J. A.; Gershenson, M. E. *Phys. Rev. Lett.* **2005**, *95*, No. 226601.

(45) Takahashi, T.; Takenobu, T.; Takeya, J.; Iwasa, Y. *Appl. Phys. Lett.* **2006**, *88*, No. 033505.

(46) (a) Kaefer, D.; Witte, G. *Phys. Chem. Chem. Phys.* **2005**, *7*, 2850. (b) Haemori, M.; Yamaguchi, J.; Yaginuma, S.; Itaka, K.; Koinuma, H. *Jpn. J. Appl. Phys.* **2005**, *44*, 3740. (c) Kafer, D.; Ruppel, L.; Witte, G.; Woll, Ch. *Phys. Rev. Lett.* **2005**, *95*, No. 166602.

(47) Käfer, D.; Ruppel, L.; Witte, G.; Wöll, Ch. *Phys. Rev. Lett.* **2005**, *95*, No. 166602.

(48) Stingelin-Stutzmann, N.; Smits, E.; Wondergem, H.; Tanase, C.; Blom, P.; Smith, P.; de Leeuw, D. *Nat. Mater.* **2005**, *4*, 601.

(49) Reichwagen, J.; Hopf, H.; Del Guerzo, A.; Belin, C.; Bouas-Laurent, H.; Desvergne, J.-P. *Org. Lett.* **2005**, *7*, 971.

(50) Hopf, H.; Reichwagen, J.; Desvergne, J.-P.; Del Guerzo, A.; Bouas-Laurent, H. *Synthesis* **2005**, 3505.

(51) Del Guerzo, A.; Olive, A. G. L.; Reichwagen, J.; Hopf, H.; Desvergne, J.-P. *J. Am. Chem. Soc.* **2005**, *127*, 17984.

(52) Chen, Z.; Muller, P.; Swager, T. M. *Org. Lett.* **2006**, *8*, 273.

(53) Takimiya, K.; Kunugi, Y.; Konda, Y.; Ebata, H.; Toyoshima, Y.; Otsubo, T. *J. Am. Chem. Soc.* **2006**, *128*, 3044.

(54) Burgdorff, C.; Kircher, T.; Loehmannsroeben, H. G. *Spectrochim. Acta, Part A* **1988**, *44A*, 1137.

(55) Hepp, A.; Heil, H.; Weise, W.; Ahles, M.; Schmechel, R.; von Seggern, H. *Phys. Rev. Lett.* **2003**, *91*, No. 157406.

(56) (a) Verlaak, S.; Cheyns, D.; Debucquoy, M.; Arkhipov, V.; Heremans, P. *Appl. Phys. Lett.* **2004**, *85*, 2405. (b) Reynaert, J.; Cheyns, D.; Janssen, D.; Müller, R.; Arkhipov, V. I.; Genoe, J.; Borghs, G.; Heremans, P. *J. Appl. Phys.* **2005**, *97*, No. 114501. (c) Santato, C.; Capelli, R.; Loi, M. A.; Murgia, M.; Cicoira, F.; Roy, V. A. L.; Stallinga, P.; Zamboni, R.; Rost, C.; Karg, S. F.; Muccini, M. *Synth. Met.* **2004**, *146*, 329.

(57) Odom, S. A.; Parkin, S. R.; Anthony, J. E. *Org. Lett.* **2003**, *5*, 4245.

(58) Campbell, R. B.; Monteath Robertson, J.; Trotter, J. *Acta Crystallogr.* **1961**, *14*, 705. For a more recent determination of the structure, see ref 27c.

(59) For an overview of polymorphism in pentacene, see: Mattheus, C. C.; Dros, A. B.; Baas, J.; Meetsma, A.; de Boer, J. L.; Palstra, T. T. M. *Acta Crystallogr.* **2001**, *C57*, 939.

(60) Siegrist, T.; Kloc, C.; Schon, J. H.; Batlogg, B.; Haddon, R. C.; Berg, S.; Thomas, G. A. *Angew. Chem., Int. Ed.* **2001**, *40*, 1732. While the device measurements performed by Schön reported in this manuscript have been discredited, the remaining authors stand behind the band structure calculations referenced in this paper.

(61) For a recent review of pentacene film growth, see: Ruiz, R.; Choudhary, D.; Nickel, B.; Toccoli, T.; Chang, K.-C.; Mayer, A. C.; Clancy, P.; Blakely, J. M.; Headrick, R. L.; Iannotta, S.; Malliaras, G. G. *Chem. Mater.* **2004**, *16*, 4497.

(62) For a recent review describing methods to optimize film morphology of organic semiconductors, see: Locklin, J.; Roberts, M. E.; Mannsfeld, S. C. B.; Bao, Z. *J. Macromol. Sci. C: Polym. Rev.* **2006**, *46*, 79.

(63) Lin, Y. Y.; Gundlach, D. J.; Nelson, S.; Jackson, T. N. *IEEE Trans. Electron Devices* **1997**, *44*, 1325.

(64) Kelley, T. W.; Muyres, D. V.; Baude, P. F.; Smith, T. P.; Jones, T. D. *Mater. Res. Soc. Symp. Proc.* **2003**, *771*, L6.5.1.

(65) Meijer, E. J.; De Leeuw, D. M.; Setayesh, S.; Van Veenendaal, E.; Huisman, B.-H.; Blom, P. W. M.; Hummelen, J. C.; Scherf, U.; Klapwijk, T. M. *Nat. Mater.* **2003**, *2*, 678.

(66) Yoo, S.; Domercq, B.; Kippelen, B. *Appl. Phys. Lett.* **2004**, *85*, 5427.

(67) Meng, H.; Bendikov, M.; Mitchell, G.; Helgeson, R.; Wudl, F.; Bao, Z.; Siegrist, T.; Kloc, C.; Chen, C.-H. *Adv. Mater.* **2003**, *15*, 1090.

(68) (a) Sakamoto, Y.; Suzuki, T.; Kobayashi, M.; Gao, Y.; Fukai, Y.; Inoue, Y.; Sato, F.; Tokito, S. *J. Am. Chem. Soc.* **2004**, *126*, 8138. (b) Inoue, Y.; Sakamoto, Y.; Suzuki, T.; Kobayashi, M.; Gao, Y.; Tokito, S. *Jpn. J. Appl. Phys.* **2005**, *44*, 3663.

(69) Sakamoto, Y.; Suzuki, T.; Kobayashi, M.; Gao, Y.; Inoue, Y.; Tokito, S. *Mol. Cryst. Liq. Cryst.* **2006**, *444*, 225.

(70) Maulding, D. R.; Roberts, B. G. *J. Org. Chem.* **1969**, *34*, 1734.

(71) Miao, Q.; Chi, X.; Xiao, S.; Zeis, R.; Lefenfeld, M.; Siegrist, T.; Steigerwald, M. L.; Nuckolls, C. *J. Am. Chem. Soc.* **2006**, *128*, 1340.

(72) Anthony, J. E.; Eaton, D. L.; Parkin, S. R. *Org. Lett.* **2001**, *4*, 15.

(73) Anthony, J. E.; Payne, M. M.; Parkin, S. R. Manuscript in preparation.

(74) Sheraw, C. D.; Jackson, T. N.; Eaton, D. L.; Anthony, J. E. *Adv. Mater.* **2003**, *15*, 2009.

(75) Martin, D. C.; Chen, J. H.; Yang, J. Y.; Drummy, L. F.; Kubel, C. *J. Polym. Sci., Part B: Polym. Phys.* **2005**, *43*, 1749.

(76) Park, S. K.; Kuo, C.-C.; Anthony, J. E.; Jackson, T. N. *2005 Int. Electron. Dev. Mtg. Technol. Digest* **2006**, 113.

(77) For a review, see: *Printed Organic and Molecular Electronics*; Gamota, D., Brazis, P., Kalyanasundaram, K., Zhang, J., Eds.; Kluwer Academic Publishers: Norwell, MA, 2004.

(78) (a) Hegmann, F. A.; Tykwinski, R. R.; Lui, K. P. H.; Bullock, J. E.; Anthony, J. E. *Phys. Rev. Lett.* **2002**, *89*, No. 227403. (b) Ostroverkhova, O.; Cooke, D. G.; Scherbyna, S.; Egerton, R.; Tykwinski, R. R.; Anthony, J. E.; Hegmann, F. A. *Phys. Rev. B* **2005**, *71*, No. 035204.

(79) Ostroverkhova, O.; Scherbyna, S.; Cooke, D. G.; Egerton, R. F.; Hegmann, F. A.; Tykwinski, R. R.; Parkin, S. R.; Anthony, J. E. *Phys. Rev. B* **2005**, *98*, No. 033701.

(80) Ostroverkhova, O.; Cooke, D. G.; Hegmann, F. A.; Tykwinski, R. R.; Parkin, S. R.; Anthony, J. E. *Appl. Phys. Lett.* **2006**, in press.

(81) Lloyd, M. T.; Mayer, A. C.; Tayi, A. S.; Bowen, A. M.; Kasen, T. G.; Herman, D. J.; Mourey, D. A.; Anthony, J. E.; Malliaras, G. G. *Org. Electron.* **2006**, *7*, 243.

(82) Swartz, C. R.; Parkin, S. R.; Bullock, J. E.; Anthony, J. E.; Mayer, A. C.; Malliaras, G. G. *Org. Lett.* **2005**, *7*, 3163.
(83) Anthony, J. E.; Swartz, C. R.; Landis, C. A.; Parkin, S. R. *Proc. SPIE* **2005**, *5940*, 2.
(84) Jiang, J.; Kaafarani, B. R.; Neckers, D. C. *J. Org. Chem.* **2006**, *71*, 2155.
(85) Payne, M. M.; Delcamp, J. H.; Parkin, S. R.; Anthony, J. E. *Org. Lett.* **2004**, *6*, 1609.
(86) Payne, M. M. Ph.D. Dissertation, University of Kentucky, Lexington, KY, May 2006.
(87) Picciolo, L. C.; Murata, H.; Kafafi, Z. H. *Appl. Phys. Lett.* **2001**, *78*, 2378.
(88) Hwang, E.-J.; Kim, Y.-E.; Lee, C.-J.; Park, J.-W. *Thin Solid Films* **2006**, *499*, 185.
(89) Wolak, M. A.; Jang, B.-B.; Palilis, L. C.; Kafafi, Z. H. *J. Phys. Chem. B* **2004**, *108*, 5492.
(90) Jang, B.-B.; Lee, S. H.; Kafafi, Z. H. *Chem. Mater.* **2006**, *18*, 449.
(91) Wolak, M. A.; Melinger, J. S.; Lane, P. A.; Palilis, L. C.; Landis, C. A.; Delcamp, J.; Anthony, J. E.; Kafafi, Z. H. *J. Phys. Chem. B* **2006**, *110*, 7928.
(92) Wolak, M. A.; Delcamp, J.; Landis, C. A.; Lane, P. A.; Anthony, J.; Kafafi, Z. *Adv. Func. Mater.* **2006**, in press.
(93) Chiang, C.-L.; Wu, M.-F.; Dai, C.-C.; When, Y.-S.; Wang, J.-K.; Chen, C.-T. *Adv. Funct. Mater.* **2005**, *15*, 231.
(94) Wex B.; Kaafarani, B. R.; Schroeder, R.; Majewski, L. A.; Burckel, P.; Grell, M.; Neckers, D. C. *J. Mater. Chem.* **2006**, *16*, 1121.
(95) Laquindanum, J. G.; Katz, H. E.; Lovinger, A. J. *J. Am. Chem. Soc.* **1998**, *120*, 664.
(96) De la Cruz, P.; Martin, N.; Miguel, F.; Seoane, C.; Albert, A.; Cano, H.; Gonzalez, A.; Pingarron, J. M. *J. Org. Chem.* **1992**, *57*, 6192.
(97) Halik, M.; Klauk, H.; Zschieschang, U.; Schmid, G.; Pnomarenko, S.; Kirchmeyer, S.; Weber, W. *Adv. Mater.* **2003**, *15*, 917.
(98) Katz, H. E.; Li, W.; Lovinger, A. J.; Laquindanum, J. *Synth. Met.* **1999**, *102*, 897.
(99) Payne, M. M.; Parkin, S. R.; Anthony, J. E.; Kuo, C. C.; Jackson, T. N. *J. Am. Chem. Soc.* **2005**, *127*, 4986.
(100) Xiao, K.; Liu, Y.; Qi, T.; Zhang, W.; Wang, F.; Gao, J.; Qiu, W.; Ma, Y.; Cui, G.; Chen, S.; Zhan, X.; Yu, G.; Qin, J.; Hu, W.; Zhu, D. *J. Am. Chem. Soc.* **2005**, *127*, 13281.
(101) Zhang, X.; Coté, A. P.; Matzger, A. J. *J. Am. Chem. Soc.* **2005**, *127*, 10502.
(102) The optimum p-stacking distance is typically regarded as within twice the van der Waals radius of carbon, or 3.4 Å or less. See also: (a) Politis, J. K.; Nemes, J. C.; Curtis, M. D. *J. Am. Chem. Soc.* **2001**, *123*, 2537. (b) Koren, A. B.; Curtis, M. D.; Francis, A. H.; Kampf, J. W. *J. Am. Chem. Soc.* **2003**, *125*, 5040.
(103) (a) Leete, E.; Ekechukwu, O.; Delvigs, P. *J. Org. Chem.* **1966**, *31*, 1967. (b) Sawtschenko, L.; Jobst, K.; Neudeck, A.; Dunsch, L. *Electrochim. Acta* **1996**, *41*, 123. (c) Riley, A. E.; Mitchell, G. W.; Koutentis, P. A.; Bendikov, M.; Kaszynki, P.; Wudl, F.; Tolbert, S. H. *Adv. Func. Mater.* **2003**, *13*, 531. (d) Choi, H.; Yang, X.; Mitchell, G. W.; Collier, C. P.; Wudl, F.; Heath, J. R. *J. Phys. Chem. B* **2002**, *106*, 1833. (e) Wudl, F.; Koutentis, P. A.; Weitz, A.; Ma, B.; Strassner, T.; Houk, K. N.; Khan, S. I. *Pure Appl. Chem.* **1999**, *71*, 295. (f) Miao, S.; Smith, M. D.; Bunz, U. H. F. *Org. Lett.* **2006**, *8*, 757. (g) Miao, S.; Bangcuyo, C. G.; Smith, M. D.; Bunz, U. H. F. *Angew. Chem., Int. Ed.* **2006**, *45*, 661.
(104) Ma, Y.; Sun, Y.; Liu, Y.; Gao, J.; Chen, S.; Sun, X.; Qiu, W.; Yu, G.; Cui, G.; Hu, W.; Zhu, D. *J. Mater. Chem.* **2005**, *15*, 4894.
(105) Miao, Q.; Nguyen, T.-Q.; Someya, T.; Blanchet, G. B.; Nuckolls, C. *J. Am. Chem. Soc.* **2003**, *125*, 10284.
(106) Wu, Y.; Li, Y.; Gardner, S.; Ong, B. *J. Am. Chem. Soc.* **2005**, *127*, 614.
(107) Li, Y.; Wu, Y.; Gardner, S.; Ong, B. S. *Adv. Mater.* **2005**, *17*, 849.
(108) Clar, E. *Polycyclic Hydrocarbons*; Academic Press: London, 1964; Vol. 1.
(109) Sirringhaus, H.; Friend, R. H.; Wang, C.; Leuninger, J.; Mullen, K. *J. Mater. Chem.* **1999**, *9*, 2095.
(110) For an excellent recent review of acenes, along with a detailed description of the issues surrounding higher acenes, see: Bendikov, M.; Wudl, F.; Perepichka, D. F. *Chem. Rev.* **2004**, *104*, 4891.
(111) Zhang, X.; Coté, A. P.; Matzger, A. J. *J. Am. Chem. Soc.* **2005**, *127*, 10502.
(112) El-Borai, M.; Abdel-Megeed, M. F.; Hassien, M.; Fahmy, M. *Sulfur Lett.* **1987**, *6*, 99.
(113) Payne, M. M.; Odom, S. A.; Parkin, S. R.; Anthony, J. E. *Org. Lett.* **2004**, *6*, 3325.
(114) See, for example: Morgenroth, F.; Berresheim, A. J.; Wagner, M.; Müllen, K. *Chem. Commun.* **1998**, 1138.
(115) Park, S.-K.; Payne, M. M.; Anthony, J. E.; Jackson, T. N. Unpublished results.
(116) Li, G.; Payne, M. M.; Anthony, J. E.; Shashidhar, R. Manuscript in preparation.
(117) This is in contrast to the carbocyclic acenes (tetracene, pentacene), which react rapidly with C_{60} in solution. See: Sarova, G. H.; Berberan-Santos, M. N. *Chem. Phys. Lett.* **2004**, *397*, 402.
(118) Payne, M. M.; Parkin, S. R.; Anthony, J. E. *J. Am. Chem. Soc.* **2005**, *127*, 8028.

CR050966Z